35 Hartwell Ave
Lexington, MA 02421

Support for Cost Analyses on Solar-Driven High Temperature Thermochemical Water-Splitting Cycles

Final Report to:
Department of Energy
Order DE-DT0000951

Report prepared by TIAX LLC
Reference D0535

February 22, 2011

Matt Kromer (Principal Investigator)
Kurt Roth
Rosalind Takata
Paul Chin

Notice:
This report was prepared as an account of work sponsored by an agency of the United States government. Neither the United States government nor any agency thereof, nor any of their employees, makes any warranty, express or implied, or assumes any legal liability or responsibility for the accuracy, completeness, or usefulness of any information, apparatus, product, or process disclosed, or represents that its use would not infringe privately owned rights. Reference herein to any specific commercial product, process, or service by trade name, trademark, manufacturer, or otherwise does not necessarily constitute or imply its endorsement, recommendation, or favoring by the United States government or any agency thereof. The views and opinions of authors expressed herein do not necessarily state or reflect those of the United States government or any agency thereof.

Any use which a third party makes of this report, or any reliance on it, or decisions to be made based on it, are the responsibility of said third party. TIAX accepts no duty or care or liability of any kind whatsoever to any such third party, and no responsibility for damages, if any, suffered by any third party as a result of decisions made, or not made, or action taken, or not taken, based on this report.

Abstract

The Department of Energy (DOE) is currently investigating approaches for producing hydrogen via solar-driven high temperature thermochemical processes (i.e., "solar thermochemical hydrogen" (STCH) production) towards an eventual goal of commercializing STCH production. The DOE has established cost targets for commercialized STCH production of $6 per kg hydrogen (2015 H_2 production cost), and $2 to $3 per kg hydrogen (2025 target for delivered H_2). In support of this effort, DOE has funded independent research teams to perform applied research on specific processes.

To help compare technologies on a consistent basis, DOE engaged TIAX to provide independent expert chemical and mechanical engineering and cost analyses support to the project teams to evaluate the cost of promising technologies. Individual process teams used chemical process flowsheet analysis to identify process conditions, major capital equipment, materials and utilities usage rates, and to estimate equipment sizes. A combination of capital equipment cost databases and bottom-up cost analysis were used to estimate costs of major capital equipment. These assumptions were applied together with a consistent set of input financial and operating assumptions that were developed jointly by TIAX and DOE to develop near-term (2015) and longer-term (2025) STCH hydrogen production cost projections. During the course of this effort, eight different STCH production processes were supported by TIAX: hybrid-sulfur (HyS), copper chloride (CuCl), thin-film nickel ferrite ("ferrite"), sulfur-ammonia (S-A), zinc oxide (ZnO), manganese oxide (MnO), sulfur-iodine (S-I), and cadmium oxide (CdO).

The resulting cost projections are summarized in Table A-1. While several of the cycles that were evaluated appear likely to achieve the near-term DOE target of $6/kg hydrogen (production only), achieving the long-term goal of $2 to $3/kg hydrogen (delivered) appears to be a very challenging prospect. Of the cycles evaluated, only one (the thin film ferrite cycle) was projected to achieve the target using base case assumptions. Even in this case, achieving the long-term target requires significant technological development along multiple dimensions, as well as demonstration and scale up of novel chemical plant concepts. Single-variable sensitivity analysis indicates that several other processes could also approach this target if more favorable economic or operational assumptions are used. While specific sensitivities vary between cycles, the plant's capacity factor, the specific economic assumptions used, cycle efficiency, and the direct capital cost were all shown to have a large effect on plant economics for each of the cycles. Heliostats costs are the primary cost driver for all of the processes that were analyzed. As such, measures that increase plant efficiency (i.e., reduce the plant thermal requirement and hence the size of the solar field) or decrease the heliostat unit cost offer a high return on investment.

Table A-1: 2015 and 2025 STCH Cost projections

Year	Hy-S	CuCl	Ferrite	S-A	ZnO	CdO[i]	MnO[ii]	S-I[iii]
2015	$5.68	$6.83	$4.06	$7.78	$6.07	N/A	$5.62	$5.01
2025	$3.85	$5.39	$2.42	$4.65	$4.18	N/A	$4.63	$4.68

[i] Validated CdO cost analysis was not completed
[ii] 2025 MnO results reflect only lower heliostat costs compared to the 2015 case
[iii] Preliminary estimate based on scaled nuclear case

TABLE OF CONTENTS

LIST OF ACRONYMS

Acronym	Meaning
ANL	Argonne National Laboratory
CdO	Cadmium Oxide STCH Cycle
Cm	centimeter
CPC	Compound Parabolic Concentrator
CSP	Concentrated Solar Power
CU	University of Colorado
CuCl	Copper Chloride STCH Cycle
DOE	United States Department of Energy
FCV	Fuel Cell Vehicle
GA	General Atomics
H2A	Hydrogen Analysis tool
HyS	Hybrid Sulfur STCH Cycle
IRR	Internal Rate of Return
Kg	Kilogram
kWh	Kilowatt hour
LHV	Lower Heating Value
M	Meter
mA	Milli-Ampere
MACRS	Modified Accelerated Cost Recovery System
MnO	Manganese Oxide STCH Cycle
MW	Megawatt
MWh	Megawatt hour
NHI	Nuclear Hydrogen Initiative
NREL	National Renewable Energy Laboratory
O&M	Operations and Maintenance
PEM	Proton Exchange Membrane
R&D	Research and Development
S&L	Sargent and Lundy (Ref 4)
S-A	Sulfur Ammonia STCH Cycle
SAIC	Science Applications International Corporation
SDE	SO_2 Depolarized Electrolyzer
S-I	Sulfur Iodine STCH Cycle
SNL	Sandia National Laboratory
SRNL	Savannah River National Laboratory
STCH	Solar Thermochemical Hydrogen
TPD	Tonnes (metric) Per Day (of hydrogen, unless otherwise noted)
US	United States of America
ZnO	Zinc Oxide STCH Cycle

1 Introduction

While hydrogen and fuel cells represent a promising pathway to reduce the environmental footprint of the United States transportation on road transportation system, in order to fully achieve these benefits, the hydrogen needs to be sourced through renewable or other domestic non-carbon emitting production pathways. One such approach is high-temperature solar thermochemical hydrogen (STCH) production. Hydrogen production from thermochemical water splitting is a chemical process that accomplishes the decomposition of water into hydrogen and oxygen using only heat or a combination of heat and electrolysis instead of pure electrolysis [1].

The U.S. Department of Energy (DOE) hydrogen program production team has established a hydrogen production cost target of $6 per kg by 2015, and a hydrogen cost target (including production and delivery) of $2 to $3 per kg by 2025 [3]. As part of the R&D effort to accomplish this goal, the DOE has funded a number of independent research teams to investigate potential cycles, select the most promising technologies, and research and develop commercially viable technology, with an eventual goal of developing a pilot STCH plant. As part of this R&D effort, DOE directed each research team to perform economic analysis to estimate the amortized hydrogen production cost for each cycle under investigation. This economic analysis aims to provide insight into the relative strengths and weaknesses of different approaches, and to identify key cost drivers.

DOE engaged TIAX to provide independent expert chemical and mechanical engineering and cost analyses support to the project teams to evaluate the cost of the most promising technologies to aid in the down-select process. The overarching goal of this activity is to help the DOE compare technologies on a consistent basis, to identify high leverage cost drivers, and to help identify a viable path for meeting long-term hydrogen program cost targets. The specific project objectives were to:

1. Provide coordination and support to the Solar-Driven High Temperature Thermochemical Project (STCH) and individual teams as they perform economic analyses for selected technologies.
2. Provide general cost estimating expertise, ensure consistency in approach, and perform peer review necessary to complete the cost assessments on an unbiased and comparable basis.
3. Contribute sound chemical and mechanical engineering expertise in the fields of concentrated solar power and thermochemical processes.

Over the course of this project, the economics of eight different STCH cycle concepts were evaluated (Table 1-1). The key figure of merit for this analysis was the projected cost of hydrogen production, on a per-kg basis, for an “Nth plant” design in the year 2015 and the year 2025. These costs were calculated from the amortized capital and operating costs for a STCH plant, which in turn were developed based on conceptual plant designs derived from chemical process flow sheet analysis. This report summarizes the results of these techno-economic analyses.

Table 1-1: Summary of DOE-funded STCH Analyses

Cycle Name	Abbreviation	Team Lead
Hybrid-Sulfur	Hy-S	Savannah River National Lab (SRNL)
Copper Chloride	CuCl	Argonne National Laboratory (ANL)
Ferrite	Ferrite	University of Colorado (CU)
Sulfur-Ammonia	SA	Science Applications International Corp (SAIC)
Zinc/Zinc Oxide	Zn/ZnO	University of Colorado (CU)
Manganese/Mn Oxide	Mn/MnO	University of Colorado (CU)
Cadmium/Cd Oxide	Cd/CdO	General Atomics (GA)
Sulfur Iodine	S-I	General Atomics (GA)

When interpreting the results of the analyses that are presented in this report, it should be noted that the technologies evaluated are at different levels of technological maturity compared to both each other, and to other previously conducted analyses of alternate hydrogen production pathways. In particular, it should be understood that pathways for the solar thermal production of hydrogen are still in the laboratory stage, while many other pathways (e.g., natural gas-to-hydrogen, coal-to-hydrogen, biomass-to-hydrogen, or low-temperature electrolysis) are in pilot or full-scale production. As such, the STCH analyses are characterized by both greater uncertainty, and in many cases, higher projected cost than other options.

To the extent possible, we have attempted to present the results of each analysis on an equal footing. However, due to constraints imposed by funding priorities and the differing maturity of the different analyses, the results presented vary in terms of both completeness and the confidence level.

This report is organized as follows: chapter 2 details the methodology employed by the individual STCH research teams and by TIAX to complete the techno-economic analysis. This is followed by an overview of the results of each of the individual STCH analyses that were conducted. The report concludes with a cross-cutting comparison of each cycle.

2 Methodology

2.1 Overview

TIAX worked with DOE and individual STCH research teams to complete the STCH techno-economic analysis using the following approach:

1. **Define the chemical process:** Individual research teams conduct applied laboratory research to define and validate the basic chemistry under real world conditions.
2. **Chemical process model:** Using chemical process modeling tools (e.g., Aspen), research teams develop an integrated thermochemical process. The goal of this step is to define material and energy flows and the process conditions for a scaled-up version of the proposed STCH cycle.
3. **Conceptual STCH plant design:** During this step, research teams identify actual equipment requirements, operational parameters, and plant integration. A solar thermal plant design capable of meeting the plant heat and energy requirements is also defined during this step.
4. **Develop cost inputs:** Cost estimates for major pieces of capital equipment, as well as fixed and variable operations and maintenance (O&M) costs are developed. While individual STCH research teams took the lead to develop these cost inputs, TIAX provided basic guidance to help ensure consistency between parallel research efforts.
5. **Conduct financial spreadsheet analysis:** Key cost inputs are used as inputs to a standardized financial spreadsheet analysis tool, which calculates the amortized cost of hydrogen production. Key assumptions for the financial analysis were developed jointly by DOE and TIAX and were applied using the DOE's H2A analysis methodology [2].
6. **Review & Revise results:** The results of the analysis are reviewed by TIAX. The process for analysis includes, but is not limited to, evaluating thermodynamics, physics laws, assumptions, flow diagrams, engineering issues under real-world conditions, and consistent financial analysis methodology. The results of this review are returned to individual teams for subsequent comment and revision.

2.2 Economic Assumptions

Each STCH research team completed their techno-economic analysis using a consistent set of input assumptions that were developed jointly by TIAX and DOE. The financial analysis uses DOE's H2A methodology – a standardized cash flow analysis spreadsheet that is widely used within the DOE's hydrogen program to improve transparency and consistency between parallel research efforts [2]. The H2A methodology uses a standardized set of plant design specifications and financial assumptions, and a standardized approach for incorporating plant capital and operating costs into analysis of project hydrogen costs (Figure 2-1).

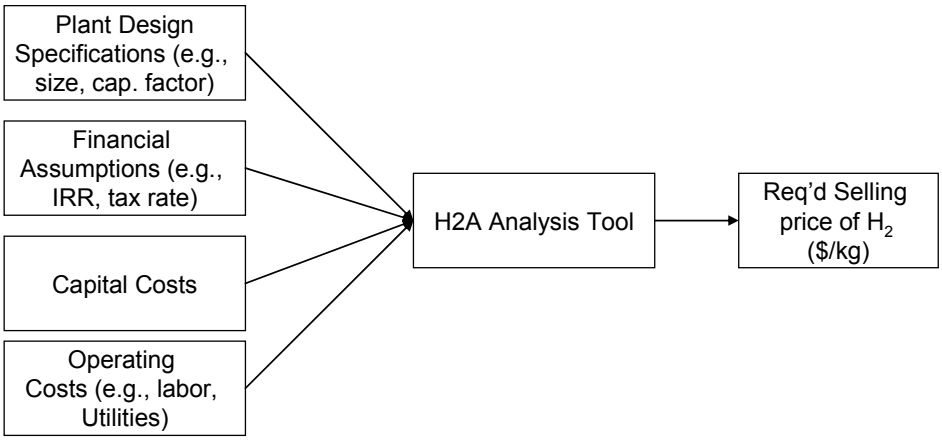

Figure 2-1: Summary of H2A analysis methodology

A summary of major design specifications specific to DOE's STCH analysis is shown in Table 2-1, while a detailed summary of the specific financial and economic assumptions used for the STCH H2A analyses is included in Appendix A.

Table 2-1: STCH Plant Design Specifications

Parameter	Specification
Plant design	Nth plant
Analysis units	Constant 2007$
Analysis years	2015 and 2025
Solar plant design point	Daggett, CA at the Spring Equinox
Solar plant capacity at design point	100 TPD H_2
Chemical plant design	133 TPD H_2
Chemical plant capacity factor	75%
Energy and feedstock	Generated onsite or purchased from renewable resources
Energy and feedstock byproduct credits	None

2.3 Efficiency

For the purposes of this analysis, two different measures of efficiency were used. These efficiency metrics provide an additional basis for comparison between cycles, and offer a valuable tool for assessing consistency between analyses.

- **STCH Process Efficiency:** The STCH process ("heat to hydrogen") energy efficiency is defined as the energy of the hydrogen produced (LHV) divided by the sum of the energy from the solar concentrator system plus any other net energy required for the process [3]. Net electricity that is consumed by the process (i.e., electricity that must be purchased) is assumed to have 40% thermal efficiency.

$$\eta_{STCH,\ Total} = \frac{E_{H2\ Prod\ (Annual\ Avg)}}{E_{th} + E_{Offsite\ Elec\ Consumer}/\eta_{Electricity}}$$

- **Solar Efficiency:** The solar ("Solar to heat") efficiency is defined as the ratio of the thermal energy available to the chemical plant to the solar energy that strikes the solar collectors:

$$\eta_{\text{Solar plant}} = \frac{E_{\text{Thermal}}}{E_{\text{Solar}}}$$

The solar plant efficiency is calculated by estimating the losses at discrete steps in the solar-to-thermal energy conversion process. This includes losses associated with collecting and concentrating solar energy (the "solar field efficiency" or "optical efficiency"), and losses associated with heat transfer and storage of thermal energy to the chemical plant (the "receiver efficiency"). A summary of the factors that contribute to solar field and receiver losses is included in Appendix B.

2.4 Cost Estimation Sources

The STCH hydrogen production cost assumptions are drawn from a variety of sources, summarized in Table 2-2. As shown, plant characteristics are divided into several categories: "performance", which includes simulation of the major material and energy flows (e.g., solar field design, chemical plant design); "financial assumptions", which include the accounting parameters used to amortize capital and operating costs over the life of the plant (e.g., inflation rate, plant life, depreciation schedule); "direct capital cost", which includes the installed cost of major pieces of equipment (e.g., compressors, heliostats); "indirect capital cost", which includes other upfront costs associated with undertaking a major capital project (e.g., site preparation, design, contingency, etc); and "operations and maintenance (O&M) cost", which include costs associated with operating and maintaining a plant over time (e.g., labor costs, fuel costs).

Table 2-2: Summary of sources and approach used to estimate STCH plant characteristics

Category	Solar Plant Guidelines	Chemical Plant Guidelines
Performance	Solar field design tool	Process modeling software (e.g., ASPEN)
Financial assumptions	H2A guidelines	H2A guidelines
Direct capital cost	- Sargent & Lundy [4] as a guideline: Solar 100 (2015) and Solar 220 (2025) used as the basis. - Scale according to plant size - Supplement with other sources on a case-by-case basis. - Heliostat costs of \$127/m^2 (2015) and 90/m^2 (2025) [6]	- Common equipment based on industry standard estimation approaches, such as CapCost [24], Peters & Timmerhaus [37], or matche.com [48] - Adjust costs of common equipment for specific temperature, pressure, and material requirements - Unique equipment on a case-by-case basis. - Electrolysis reactor approach summarized in Appendix B
Typical scaling factor[1]	1.0 – field sizing 0.7 – other solar field equipment	0.6
Indirect capital cost	Sargent & Lundy	Turton, H2A guidelines
O&M cost	Sargent & Lundy	Turton, H2A guidelines

Solar plant specifications rely primarily on the approach used by Sargent & Lundy's 2003 [4] study of concentrated solar power (CSP), while chemical plant specifications rely primarily on the approach used by Turton et al [5] to estimate chemical plant costs. Heliostat costs are based on a recent heliostat cost reduction study conducted by Sandia National Laboratory [6]. Both the solar and chemical plant modules also draw on common H2A assumptions. Other sources and

[1]This refers to the exponent (n) used to scale equipment costs for differing size specifications. The relationship between size (S) and cost (C) for two different plants is given by: $C_1/C_0 = (S_1/S_0)^n$.

alternative assumptions may be used as appropriate, with the caveat that these sources should be made available for review and use appropriate methodology. A brief description of some of the critical assumptions and sources is included in Appendix A.

2.5 Sensitivity Analysis

Analysis of several of the STCH cycles includes single variable sensitivity analysis to assess the effect of varying critical assumptions on the cost analysis. Several parameters were varied in a consistent fashion for each project, while others were evaluated on a case-by-case basis. A summary of the widely used sensitivity parameters is shown in Table 2-3.

Table 2-3: Sensitivity Analysis Overview

Parameter	Range of Values
Heliostat cost	2015: \$120 to \$160/m^2 (\$127/m^2 base) ; 2025: \$80 to \$120/m^2 (\$90/m^2 base)
Capacity Factor	60 to 80% (75% base)
Economic assumptions	Base Case: H2A standard financial calculation parameters S&L assumptions: Uses assumptions consistent with the Sargent & Lundy economic analysis[2]
Cost of Electricity	2015: \$0.068 to \$0.097/kWh (\$0.083 base); 2025: \$0.048 to \$0.068/kWh (\$0.058 base)
Capital Cost	Case-by-case, with specific evaluation of high-risk components
Efficiency	Adjust on a case-by-case basis
Labor	Adjust on a case-by-case basis

[2] The following adjustments are made to the H2A values: 10% Investment Tax Credit (vs. 0%), 11.5% Real IRR (vs. 10%), 5 yr MACRS (vs. 20), 50% equity (vs. 100%), 20 yr debt (vs. NA), 8.5% debt rate (vs. NA), 1 yr construction (vs. 3), 30 yr life (vs. 40), 2.5% inflation (vs. 1.9), 8% State Tax (vs. 6%), Prop Tax/Ins non-solar property 1% (vs. 2%).

3 Results

3.1 Overview of Solar Thermal Water Splitting

The following section provides an overview of the basic chemistry, the plant design concept, the major cost inputs, and the projected hydrogen selling price for each of the STCH cycle evaluations that were completed during the course of this project.

Due to factors such as funding constraints and differing project timelines, not all of the STCH research efforts resulted in completed, validated H2A economic analyses to allow a true "apples to apples" comparison with other systems. The status of the various STCH analyses is summarized in Table 3-1: as shown, research on three of the analyses (CuCl, ferrite, and S-A) is currently ongoing; three others were largely completed but included several minor inconsistencies (Hy-S, ZnO, and MnO). The remaining two (CdO, S-I) ran out of funding before validated cost analyses could be completed. For the three cycles that required minor revisions, we have presented modified results that seek to account for these inconsistencies. For the two incomplete analyses, we have provided a qualitative summary of major process characteristics, but do not believe that the economic analysis was mature enough to provide a fair comparison to the other systems in their current state.

Table 3-1: Status of STCH cycle H2A analysis

Cycle	Process Flowsheet Optimization	Status of H2A Economic Analysis
Hy-S	Completed, Oct 2008	Completed, Oct 2008; required minor revisions
CuCl	Ongoing	Ongoing, reviewed Jan 2011
Ferrite	Ongoing	Ongoing, reviewed Jan 2011
S-A	Ongoing	Ongoing, preliminary analysis reviewed, Jan 2011
Zn/ZnO	Completed, Oct 2008	Completed, Oct 2008; required minor revisions
Mn/MnO	Completed, Oct 2008	Final analysis partially reviewed by TIAX
S-I	Completed, Oct 2008	Final analysis not reviewed by TIAX
Cd/CdO	Completed, Oct 2008	Incomplete

3.2 Hybrid-Sulfur STCH Process

3.2.1 Overview

The analysis of the hybrid-sulfur (Hy-S) water splitting cycle presented here was conducted by Savannah River National Laboratory (SRNL) and builds on a wide body of research into this and similar processes [7,8,9]. The hybrid-sulfur process involves two chemical reactions, summarized in Table 3-2. The first reaction is the thermal decomposition of sulfuric acid, which occurs at 800 to 900 C. Catalyst development for the decomposition reaction is ongoing and is critical to obtain suitable kinetics. The second stage is the decomposition of water, which occurs electrochemically at 80 to 120 C and entails reacting sulfur dioxide and water to form hydrogen and sulfuric acid. The cycle is attractive compared to water electrolysis because the SO_2 electrolysis is significantly less energy intensive [10, 11].

Table 3-2: Hybrid-Sulfur Cycle Reaction Summary

Stage	Net Reaction	Notes/Comments
Decomposition of H_2SO_4	$H_2SO_4 \rightarrow 0.5O_2 + SO_2 + H_2O$	Occurs thermochemically in a bayonet heat exchanger at approximately 800 to 900 C
Decomposition of water	$SO_2 + 2H_2O \rightarrow H_2 + H_2SO_4$	Occurs electrochemically at 80 to 120 C

3.2.2 Plant Design

The hybrid-sulfur process utilizes thermal energy to drive the decomposition of sulfuric acid, and electricity to power the hydrogen-producing electrolysis reaction and to power plant auxiliaries (Figure 3-1). Approximately 78% of the energy is sourced from solar thermal energy, and 22% from electricity. Solar thermal energy is collected using a particle receiver mounted on a solar power tower and stored in a hot sand storage medium to enable 24-hour plant operation and minimize plant start-ups (Figure 3-2). The solar field was designed using DELSOL, a solar plant optimization tool developed by SNL [12]. The key solar field design parameters are summarized in Table 3-3. As shown, due to improvements in the chemical plant efficiency (discussed below), the 2025 solar plant has a significantly smaller heliostat field and only requires a single power tower.

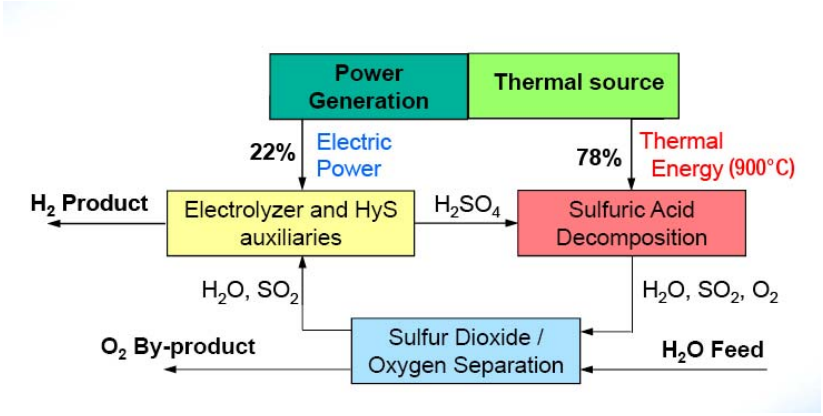

Figure 3-1: Summary of Hybrid-Sulfur unit operations [13]

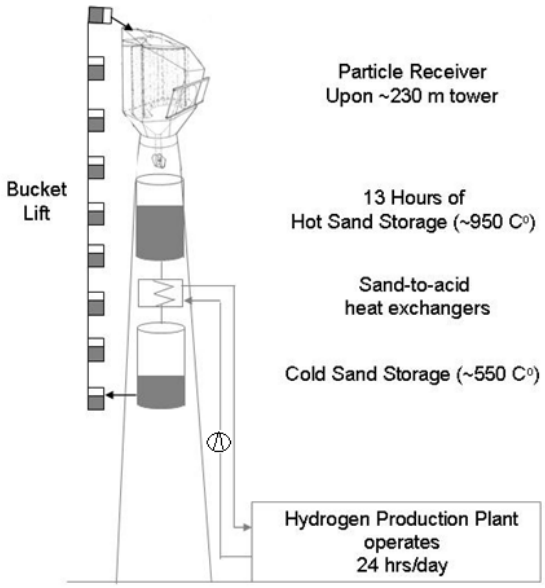

Figure 3-2: Conceptual diagram of Hybrid-Sulfur Receiver/Tower concept [14]

Table 3-3: Summary of Hy-S solar plant operational characteristics

Parameter	2015	2025
Design point (TPD H_2)	100	100
Heliostat area (m^2)	1,717,000	1,370,000
Tower height (m)	230	340[3]
Number of towers	2	1
Number of solar fields	2	1
Solar field efficiency	46%	46%[4]
Solar auxiliaries (MW_e)	1.1 kWh/kg H_2	1.1 kWh/kg H_2
Thermal Storage	Alumina sand, 4,300 MWth	Alumina sand, 3,400 MWth
Max temperature	1,000 C	1,000 C
Receiver (MW_{Th}, peak)	890, particle receiver	702

The hybrid-sulfur chemical plant design is based on detailed analysis prepared by Shaw, Stone, and Webster [10, 11, 14] in collaboration with SRNL and Westinghouse as part of an evaluation of a nuclear-driven hybrid-sulfur process. The nuclear-driven hybrid-sulfur process differs from the solar-thermal process primarily insofar as the thermal energy source and the plant's design point capacity differ. Additional minor adjustments were made to plant costs to reflect differences in the nuclear versus solar plant layout. Subsequent analysis by SRNL using an alternate costing approach led them to conclude that a number of the cost estimates for standard capital equipment were conservative, so some of the costs from the Shaw report were adjusted downward.

The core elements of the chemical plant (Figure 3-3) are a sulfur decomposition reactor and an SO_2-depolarized electrolyzer (SDE). The balance of plant includes an H_2SO_4 concentration stage (using a flash reactor and a vacuum column) at the decomposition reactor feed, a gas

[3] It should be noted that this tower height is significantly taller than those evaluated in the Sargent & Lundy study
[4] The 2025 plant uses a significant larger field but has the same solar efficiency as the 2015 field. This seems to be a questionable assumption

separation stage to remove the oxygen waste from the decomposed H_2SO_4 outlet, and a mixing tank to feed the SDE. It also includes heat exchangers to supply thermal energy from the hot sand storage medium. The decomposition reactor utilizes a novel bayonet reactor design made of silicon carbide, which is resilient to H_2SO_4 at high temperature and pressure (Figure 3-4). The reactor is designed to recuperate thermal energy internally using a counterflow arrangement, which has the benefit of low temperature streams at the inlet and outlet, thereby enabling low cost seals. The reactor requires successful development of a decomposition reactor catalyst, as well as demonstration of reliability and heat transfer at scale.

The SDE is based on proton exchange membrane (PEM) technology that is designed to meet the requirements imposed by the concentrated H_2SO_4 solution (Figure 3-4). The electrolyzer is assumed to operate at 21 bar, and deliver 600 mA/cm^2 at 0.6 V, with a 5 (2015 case) to 10 (2025 case) year lifetime. At present, an SDE electrolyzer (single cell) has been successfully tested in the laboratory to 0.76 V and 1,100 mA/cm^2 at 6 bar over short durations. In addition, an electrolyzer membrane that prevents SO_2 diffusion needs to be demonstrated [15].

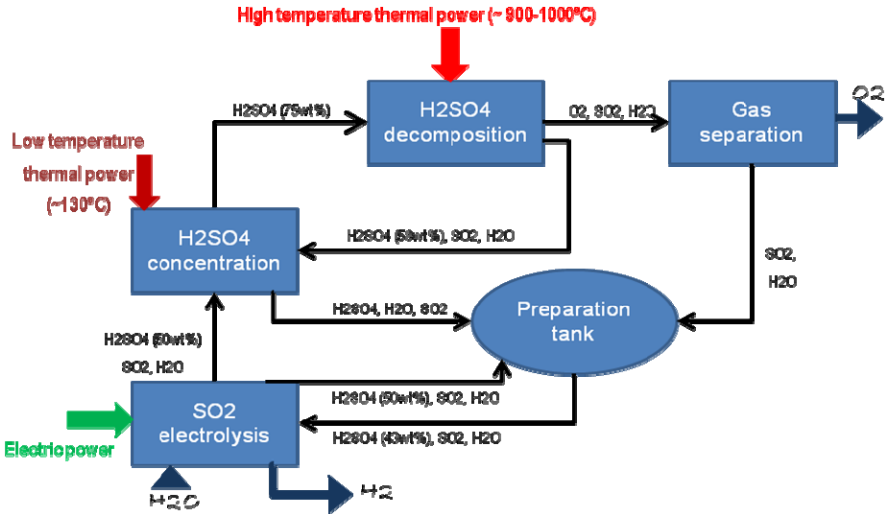

Figure 3-3: HyS plant block diagram [14]

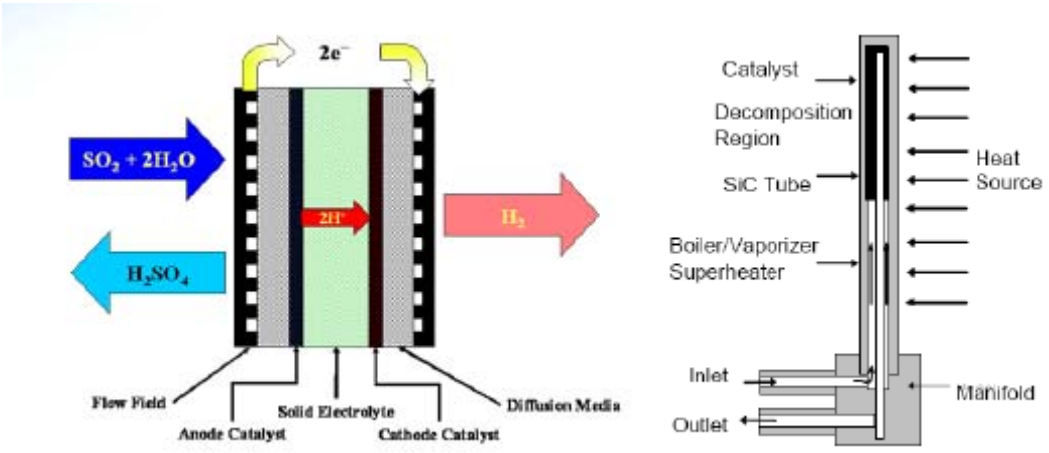

Figure 3-4: SO_2-depoloarized electrolyzer (left) and bayonet sulfur decomposition reactor (right) [14]

A summary of the key hybrid-sulfur 2015 and 2025 chemical plant operational characteristics is shown in Table 3-4. Compared to the 2015 plant, the 2025 plant includes an improved flowsheet arrangement, a higher efficiency electrolyzer system, and the elimination of an intermediate heat transfer loop between the hot sand thermal storage and the decomposition reactor. The 2025 plant's lower electrical and thermal power requirement thereby improve the STCH efficiency from 32% in 2015 to 39% in 2025.

Table 3-4: Summary of Hy-S chemical plant operational characteristics

Parameter	2015	2025
Design point (TPD H_2)	133.4	131.6
Max temperature	900	900
# of reactions	2	2
Sulfur Decomposition	Bayonet reactor w/intermediate heat exchange	Bayonet reactor w/direct heat exchange
Electrolysis	0.6 V, 500 mA/cm^2	0.5 V, 500 mA/cm^2
Electrolyzer Refurbishment[5]	40,000 hrs (5 yrs)	80,000 hrs (10 yrs)
Duty cycle (hrs per day)	24	24
Thermal energy use	334 MW_{th}	260 MW_{th}
Electrolyzer energy use	16 kWh/kg H_2	13.9 kWh/kg H_2
Auxliary energy use	1.4 kWh/kg H_2	0.5 kWh/kg H_2
# of laborers (solar + chem)	49	35
STCH efficiency[6]	32%	39%

3.2.3 Cost Assumptions

The major capital and operating costs are summarized in Table 3-5. The hybrid-sulfur chemical plant costs are based on the detailed cost analysis included in the Shaw report [10] discussed above. To apply the costs to the solar-to-hydrogen case, costs were scaled for the plant size[7] and adjusted to year 2007$. Because a number of the STCH baseline assumptions have evolved since the completion of the hybrid-sulfur STCH H2A analysis in 2008, it was necessary for TIAX to make several adjustments to the cost analysis originally performed by SRNL.[8] The performance improvements from 2015 to 2025, coupled with reductions in electrolyzer component costs and improvements in the electrolyzer durability result in significantly lower capital and operating costs for the 2025 plant.

[5] Incurs refurbishment costs of 60% of the initial installed capital cost
[6] See section 2.3 for the definition of the STCH efficiency
[7] A scaling exponent of 0.55 to 0.6 for chemical plant components, and 0.7 for solar equipment
[8] These adjustments included updating costs from 2005$ to 2007$, modifying several of the indirect cost inputs, and adjusting the capital cost of the electrolyzer (2015 only) and thermal storage to align with the other, more recent analyses.

Table 3-5: Hybrid-Sulfur capital and operating costs

Category	2015	2025	Comments
Solar Plant Installed Capital Costs			
Heliostats	$217	$126	$127.5/m^2 (2015), $90/m^2 (2025) [6]
Receivers	$19	$11	Falling sand receiver, scaled from [16]
Towers/Piping	$27	$33	2 230m (2015) / 1 340m (2025) tower [4]
Thermal Storage	$86	$68	$20/kWh [17,18,19]
Controls	$2	$2	[4]
Balance of Plant	$24	$20	Scaled from [4]
Total Solar Cost	**$375**	**$259**	**Sum of the above**
Chemical Plant Installed Capital Costs			
Sand-to-He loop	$18	$0	Intermediate heat exchange loop eliminated for 2025 design
Decomposition reactor and balance of reactor	$89	$92	Scaled from [10]
Feed and utility supply	$7	$7	Scaled from [10]
SO2 Electrolyzer AND Balance of electrolyzer	$55	$36	Electrolyzer module costs as discussed in App C; balance of system costs from [10]
Chemical Plant Cost	**$169**	**$135**	Sum of the above
Chemical Plant Installed Capital Costs			
Total Direct Capital	$543	$394	Sum of chemical & solar plant cost
Indirect Capital	$187	$138	Includes contingency, fees, engineering & design, site preparation, and land cost
Total Capital Cost	**$730**	**$532**	Sum of indirect & direct capital
Annual Operating Cost			
Fixed op costs	$25	$19	Includes labor, prop taxes, insurance, maintenance & repairs.
Variable op costs	$56	$34	Includes electricity & water
Total Operating Cost	**$81**	**$53**	**Sum of fixed and variable operating costs**

3.2.4 Results

A summary of the hydrogen cost projected by the hybrid-sulfur H2A analysis is shown in Table 3-6. As shown, the 2015 case is projected to achieve the near-term target of $5 to $6 per kg, while the 2025 case is higher than the long-term target of $2 to $3 per kg. The major contributor to the hydrogen selling price is the plant capital cost (approximately 60% of the total). As shown in Table 3-5, the bulk of the direct capital expense consists of the solar plant, for which the heliostats are the primary cost driver. Utilities, which are primarily a function of the purchased electricity needed to power the electrolysis reactor, also comprise a significant fraction of the total hydrogen costs (approximately 25%).

Table 3-6: Hybrid-Sulfur Cost Breakdown

Analysis Year	Capital	Fixed O&M	Var O&M	Total	Critical Assumptions
2015	$3.43	$0.70	$1.54	**$5.68**	- Electrolyzer module uninstalled cost of ~$520/$kW_e$ - 0.6 V, 500 mA/cm^2 electrolyzer operation - 5 yr electrolyzer lifetime - Suitable catalyst development - $127/$m^2$ heliostat cost
2025	$2.38	$0.54	$0.92	**$3.85**	- Electrolyzer module uninstalled cost of $300/$kW_e$ - 0.5 V, 500 mA/cm^2 electrolyzer - 10 yr electrolyzer lifetime - Suitable catalyst development - Elimination of intermediate heat transfer - $90/$m^2$ heliostat cost

Single-variable sensitivity analysis was conducted on major input assumptions. The results of this analysis are shown in Figure 3-5 (2015) and Figure 3-6 (2025). The capacity factor has a large affect on the upper bound projected cost of hydrogen, while the alternate financial assumptions have a large affect on the lower bound; uncertainty in the capital cost is also important.

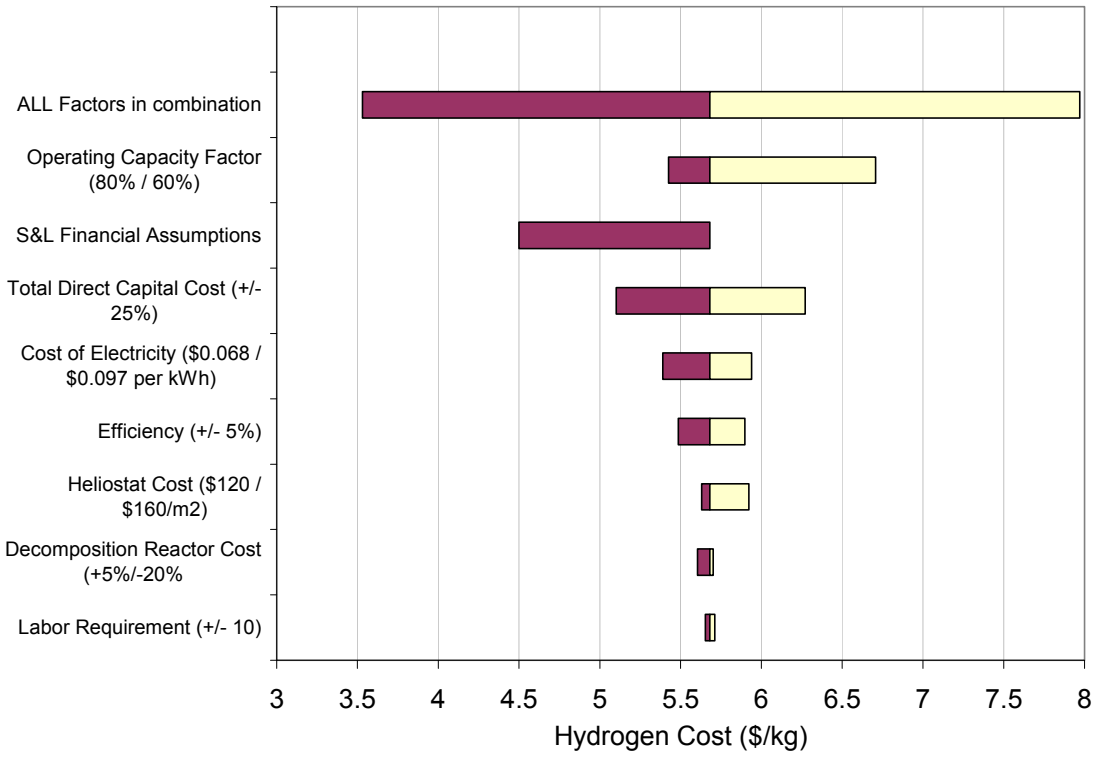

Figure 3-5: Single-variable sensitivity analysis, Hy-S 2015 case

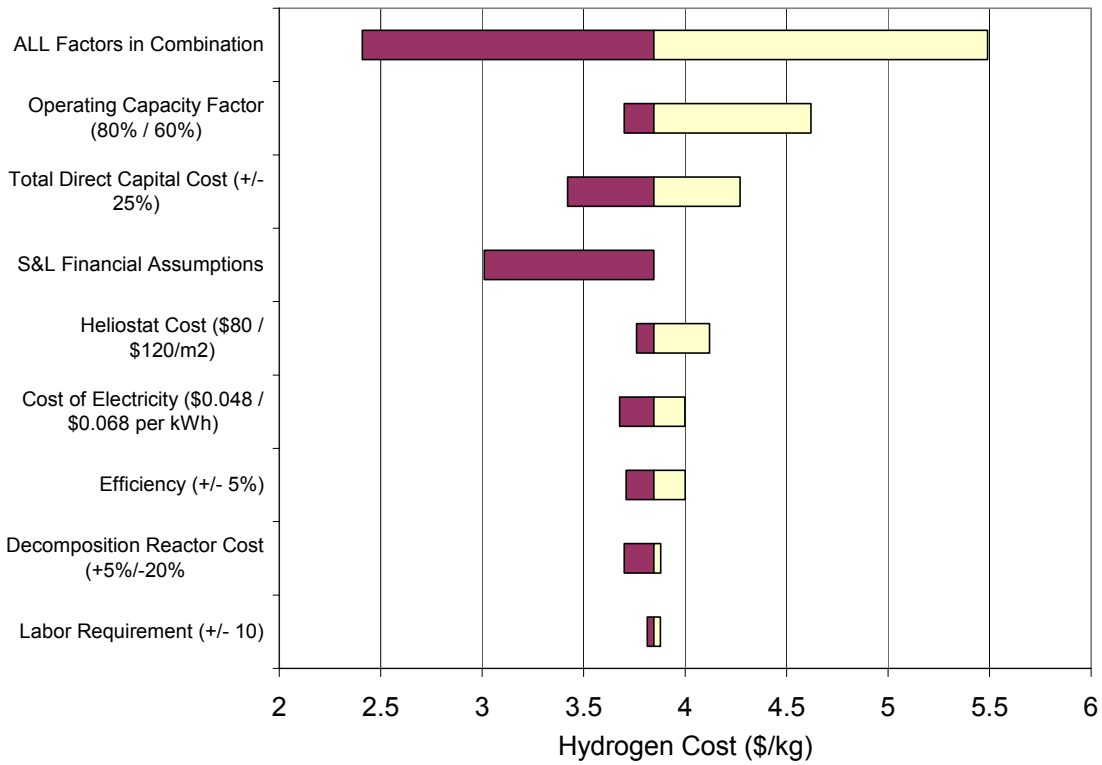

Figure 3-6: Single-variable sensitivity analysis, Hy-S 2025 case

3.3 Copper Chloride (CuCl) STCH Process

3.3.1 Cycle Description

The analysis of the copper chloride water splitting cycle presented here was conducted by a team led by Argonne National Laboratory (ANL). The hybrid copper chloride cycle is a 3-step chemical process, summarized in Table 3-7. The process includes an oxygen generation step, which occurs at 550 C and 1 bar, followed by the crystallization and hydrolysis of $CuCl_2$ at 400 C and 1 bar. The cycle is completed with the electrolysis of CuCl and HCl at 100C and 24 bar, during which the hydrogen product is evolved [20,21].

Table 3-7: Summary of CuCl Cycle

Stage	Net Reaction	Notes/Comments
Oxygen generation	$Cu_2Cl_2O \rightarrow 2CuCl + .5O_2$	Thermal decomposition of copper oxychloride: 550 C and 1 bar. Molten CuCl is produced.
Hydrolysis of $CuCl_2$	$2CuCl_2 + H_2O \rightarrow 2HCl + Cu_2Cl_2O$	Crystallization of $CuCl_2$ (55 C, 24 bar) followed by hydrolysis to Cu_2OCl_2 (400 C, 1 bar) in a large excess of water
Electrolysis	$2CuCl + 2HCl \rightarrow H_2 + 2CuCl_2$	Electrolysis at 100 C and 24 bar

While the individual steps of the CuCl process have been independently validated, the intermediate separation steps have not all been demonstrated, and the complete cycle has not been closed. Other key challenges to successfully deploying the system relate to: (1) successfully integrating each of the process steps while maintaining process efficiency; and (2) developing a durable electrolysis membrane that minimizes copper crossover [22].

3.3.2 Plant Design

A high level conceptual design of the plant is shown in Figure 3-7. As shown, solar thermal energy is concentrated from heliostat fields onto a molten salt receiver mounted on a solar power tower and stored in a molten salt storage medium to enable 24-hour operation of the hydrogen production plant. The thermal energy drives the decomposition of copper oxychloride and the hydrolysis of cuprous chloride, while electricity powers the hydrogen-producing electrolysis reaction and the plant auxiliaries. Approximately 20 to 25% of the energy is sourced from electricity, and 75 to 80% from solar thermal energy. The solar field was designed using DELSOL [12]. Key solar field design parameters are summarized in Table 3-8.

A process flowsheet for the CuCl chemical plant was developed using Aspen Plus. The core elements of the copper chloride chemical plant include hydrolysis reactors, oxychloride decomposition reactors, crystallizers, and an electrolyzer system. With the exception of the electrolyzer system, these process steps are similar to commercially practiced technologies, and are sized according to residence times observed in the laboratory. A flow diagram of each of the primary unit processes in the CuCl cycle is shown in Figure 3-8. The electrolyzer anode feed pumps an aqueous solution of CuCl at 24 bar and 100 C through the anode where the CuCl reacts with chloride ions from the cathode to form $CuCl_2$. The solution is cooled in a crystallizer and collected in a hydrocyclone, from which it feeds into the hydrolysis reactor. The hydrolysis reactor is a spray roaster, similar to units used in the steel industry. Solid $CuCl_2$ is sprayed into the reactor, which contains a large excess of superheated steam at 400 C, 0.25 bar, during which

copper oxychloride is formed. Energy to vaporize the steam is provided by stored solar thermal energy. The copper oxychloride is then decomposed in a bayonet-style reactor into molten CuCl and oxygen at 550 C. After recovering heat from the molten CuCl, it is returned to the anode feed. The electrolyzer cathode feed is an aqueous HCl solution at 24 bar and 100 C. As the HCl solution passes through the cathode, Cl^- migrates to the anode, and hydrogen is evolved. The cathode feed is then cycled through a flash reactor: vaporized steam from the flash feeds the hydrolysis reactor and remaining liquid is recycled to the cathode feed. Critical cycle characteristics are summarized in Table 3-9 [20, 21, 23].

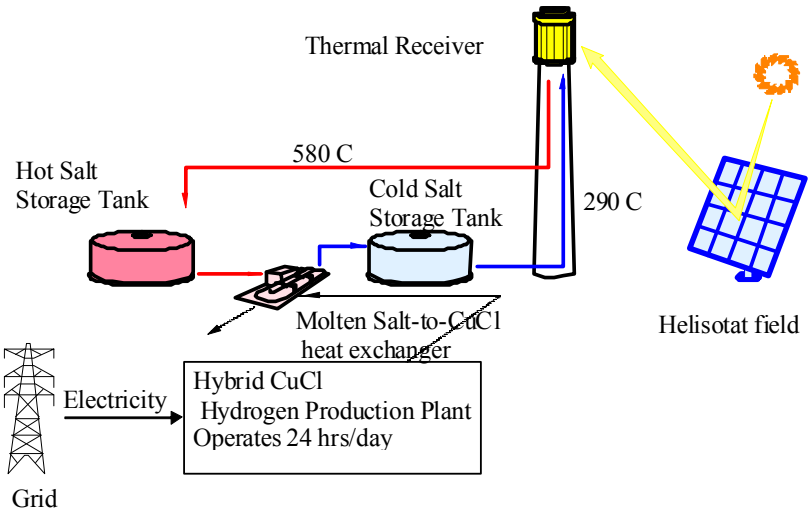

Figure 3-7: Copper chloride plant configuration [23]

Table 3-8: Summary of CuCl solar plant operational characteristics

Parameter	2015	2025
Design point (TPD H_2) [9]	93.75	93.75
Heliostat area (m^2)	1,779,000	1,779,000
Tower height (m)	190	190
Number of towers	2	2
Number of solar fields	1 per tower	1 per tower
Solar-to-heat efficiency[10]	49%	49%
Solar auxiliaries	0.3 kWh/kg H_2	0.3 kWh/kg H_2
Thermal Storage	Molten Salt, 4,420 MWh_{th}	Molten Salt, 4,420 MWh_{th}
Max temperature	580 C	580 C
Receiver	460 MW_{th}	460 MW_{th}

The electrolyzer is assumed to operate at 0.7V, 500 mA/cm^2 (2015 case), and to improve to 0.63V, 500 mA/cm^2 (2025 case), and require refurbishment every five (2015) to ten (2025) years. Electrolyzer operation has been demonstrated to 0.7 and 100 mA/cm^2. Due to the corrosive environment, all of the major pieces of equipment are assumed to include a porcelain lining. This coating is anticipated to address any materials of construction issues, but this assumption has not yet been validated. As currently conceived, the CuCl cycle suffers from relatively low thermal efficiency, which necessitates a large heliostat field. This low efficiency is primarily a

[9] The CuCl analysis was conducted for a plant with a peak capacity of 125 TPD hydrogen – not 133 TPD, as was the case for other analyses. The minor difference in plant size would not materially affect the results of the analysis.
[10] See section 2.3 for definition of solar-to-heat efficiency

function of the energy needed to vaporize the hydrolysis feed water. There may be opportunities to reduce the cycle's thermal requirement through improved heat integration, but these approaches are still under investigation [22].

Table 3-9: Summary of CuCl chemical plant operational characteristics

Parameter	2015	2025
Design point (TPD)	125	125
Max temperature	540	540
# of reactions	3	3
Oxychloride Decomp. Reactor	Bayonet-style heat exchanger	Bayonet-style heat exchanger
Electrolysis Reactor	PEM Elecctrolyzer: 27,000 m^2, 0.7 V, 500 mA/cm^2	PEM Elecctrolyzer: 27,000 m^2, 0.63 V, 500 mA/cm^2
Electrolyzer Refurbishment[11]	5 years	10 years
Hydrolysis Reactor	Spray roaster	Spray roaster
Duty cycle (hrs per day)	24	24
Thermal energy use	65 kWh/kg H_2	65 kWh/kg H_2
Electrolyzer energy use	18.6 kWh/kg H_2	16.8 kWh/kg H_2
Auxiliaries energy use	1.1 kWh/kg H_2	1 kWh/kg H_2
# of laborers (solar + chem)	100	100
STCH efficiency[12]	29%	30%

[11] Refurbishment costs of 60% of the initial installed capital cost are required for the electrolyzer at the end of life
[12] See section 2.3 for definition of solar-to-heat efficiency

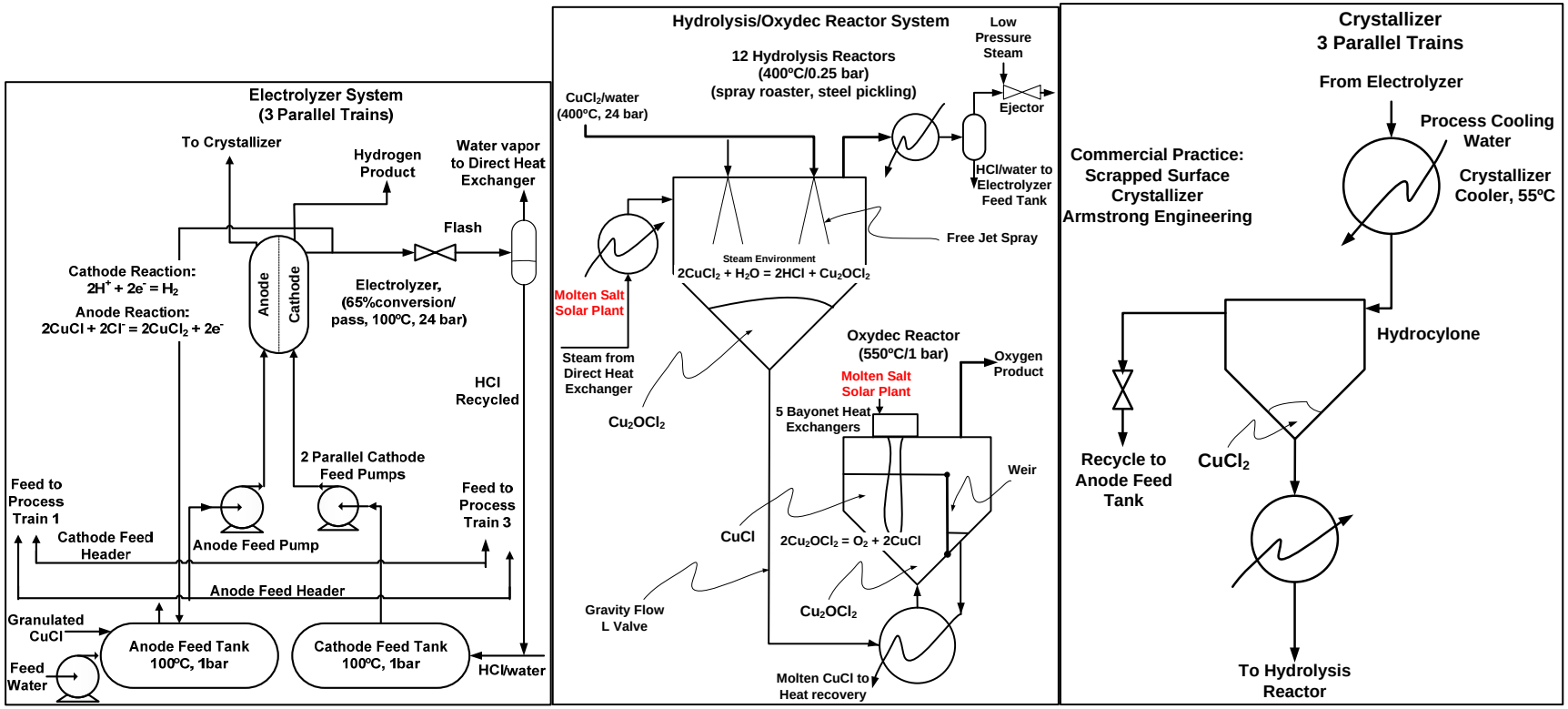

Figure 3-8: Illustrative flow diagrams for major capital equipment for the copper chloride plant – (left to right): Electrolyzer system, Hydrolysis/Decomposition Reactor; and Crystallizer [23]

3.3.3 Capital and Operating Cost Estimates

With the exception of the electrolysis unit, the CuCl chemical plant uses standardized plant equipment that is similar to equipment used in present-day chemical processes. Chemical plant equipment costs were estimated primarily using CAPCOST cost estimation software [24]. To handle the corrosive environment, major equipment was assumed to be constructed of carbon steel and coated with a porcelain lining, which was assumed to add 20 to 25% to the installed equipment cost [25]. As shown, the heliostat costs are the primary cost driver for the total system cost. The key cost drivers for the chemical plant are the reactors, electrolysis unit, and heat integration. The CuCl plant requires significant electricity to drive the electrolysis reaction, and, due to the large number of solids handling steps, has a relatively large labor requirement.

Table 3-10: CuCl STCH cycle capital and operating costs

Category	2015	2025	Comments
Solar Plant Installed Capital Costs			
Heliostats	$224	$160	$127.5/m^2 (2015), $90/m^2 (2025) [6]
Receivers	$64	$64	Molten salt receivers, scaled from [4]
Towers/Piping	$18	$18	2 190m towers, scaled from [4]
Thermal Storage	$88	$88	$20/kWh$_t$ [17,18,19]
Controls	$2	$2	[4]
Balance of Plant	$24	$20	Scaled from [4]
Total Solar Cost	**$421**	**$353**	**Sum of the above**
Chemical Plant Installed Capital Costs			
Heat Exchangers	$32	$29	CAPCOST, porcelain lined [24, 25]
Pumps	$4	$4	CAPCOST, porcelain lined [24, 25]
Pressure Vessels (Reactors)	$52	$39	Includes hydrolysis reactor, decomposition reactor, crystallizers, and cyclones, etc CAPCOST, porcelain lined [24, 25]
Storage Tanks	$0.3	$0.3	CAPCOST, porcelain lined [24, 25]
Compressors	$15	$16	CAPCOST, porcelain lined [24, 25]
Steam generation	$5	$5	CAPCOST, porcelain lined [24, 25]
Balance of Chemical Plant	$36	$31	Estimated from Turton & Hall [5]
Initial Chemical Inventory	$10	$8	486 MT of HCl at $241/MT; 1,076 MT (2015)/909 MT (2025) of CuCl at $7200/MT
Electrolysis Reactor System	$38	$32	Active area = 27,700 m^2; $1,140/m^2 (2015), $950/m^2 (2025) x 1.2X inst factor. See App C.[13]
Chemical Plant Cost	**$192**	**$163**	**Sum of the above**
Chemical Plant Installed Capital Costs			
Total Direct Capital	$612	$516	Sum of chemical & solar plant cost
Indirect Capital	$208	$178	Includes contingency, fees, engineering & design, site preparation, and land cost
Total Capital Cost	**$821**	**$694**	Sum of indirect & direct capital
Annual Operating Cost			
Fixed op costs	$36	$33	Includes labor, prop taxes, insurance, maintenance & repairs.
Variable op costs	$59	$38	Includes electricity & water
Total Operating Cost	**$95**	**$71**	**Sum of fixed and variable operating costs**

[13] Some components of the electrolysis reactor balance of plant are included elsewhere in the cost estimates.

3.3.4 Results

A summary of the hydrogen cost projected by the CuCl H2A analysis is shown in Table 3-11. As shown, the 2015 case exceeds the near-term target of $5 to $6 per kg, and the 2025 case is significantly higher than the long-term target of $2 to $3 per kg. The major contributor to the hydrogen selling price is the plant capital cost (approximately 60% of the total), which in turn is a function of the cycle's relatively low process efficiency. Utilities, which are primarily a function of the purchased electricity needed to power the electrolysis reactor, also comprise a significant fraction of the total hydrogen cost (approximately 20 to 25%).

Table 3-11: CuCl Cost Breakdown

Analysis Year	Capital	Fixed O&M	Var O&M	Total	Critical Assumptions
2015	$4.00	$1.09	$1.74	**$6.83**	- Electrolyzer module uninstalled cost of $1,140/$m^2$ - 0.7 V, 500 mA/cm^2 electrolyzer - Corrosive environment addressed with porcelain-lined equipment - 5 yr electrolyzer lifetime - $127/$m^2$ heliostat cost - 29% cycle efficiency
2025	$3.30	$0.98	$1.11	**$5.39**	- Electrolyzer module uninstalled cost of $950/$m^2$ - 0.63 V, 500 mA/cm^2 electrolyzer - Corrosive environment addressed with porcelain-lined equipment - 10 yr electrolyzer lifetime - $90/$m^2$ heliostat cost - 30% cycle efficiency

Single-variable sensitivity analysis was conducted on major input assumptions. The results of this analysis are shown in Figure 3-9 (2015) and Figure 3-10 (2025). As shown, even with improvements along multiple dimensions, it will be challenging for the CuCl cycle to achieve the long term targets. Improvements in the process efficiency may be feasible with improved heat integration and other process optimization steps. If realized, they would significantly reduce the plant capital costs in several respects: (1) The solar plant would require a smaller heliostat field, reactor, and less thermal storage. Depending on the degree of efficiency improvement, the plant could potentially be deployed as a single field, which would also reduce tower and reactor costs; and (2) The chemical plant would require smaller reactors – in particular, smaller flash units, which constitute a major portion of the total capital cost.

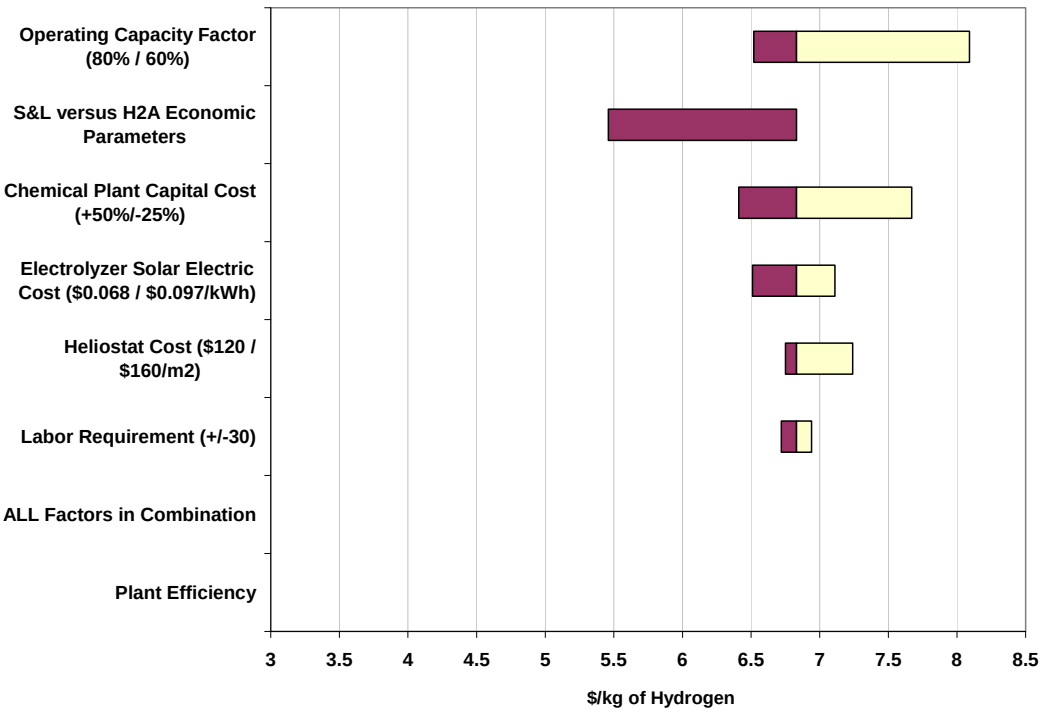

Figure 3-9: Single-variable sensitivity analysis, CuCl 2015 case

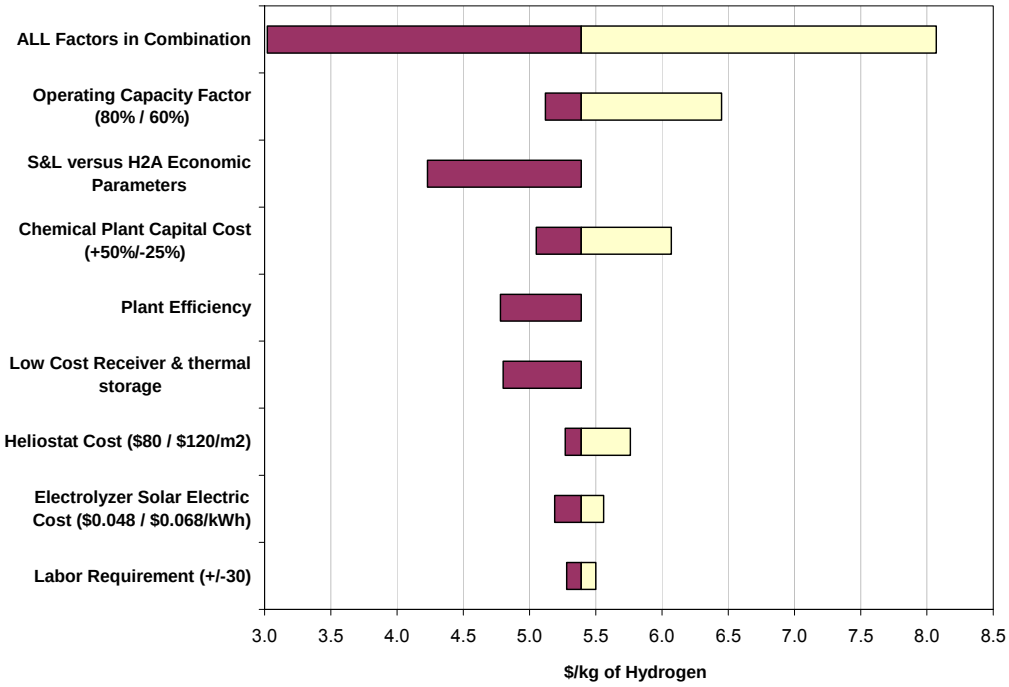

Figure 3-10: Single-variable sensitivity analysis, CuCl 2025 case[14]

[14] The low cost receiver and thermal storage case assumes: (1) a cost similar to the falling sand receiver used in the hybrid-sulfur analysis; and (2) $10/kWh thermal storage.

3.4 Ferrite STCH Process

3.4.1 Cycle Description

The analysis of the ferrite water splitting cycle presented here was conducted by a University of Colorado (CU) research team. The ferrite cycle investigated for detailed economic analysis is based on the thermal reduction of nickel ferrite ($NiFe_2O_4$). This cycle is a two-step process, summarized in Table 2-2. The first step entails the reduction of nickel ferrite to a metal oxide ($Fe^{2+} + Fe^{3+} + Ni^{2+}$) at temperatures on the order of 1,450 C, during which oxygen is evolved; this is followed by the oxidation of metal oxide back to nickel ferrite at lower temperature (on the order of 1,000 C), during which hydrogen is evolved. The operating temperatures of the two steps were selected to maximize the equilibrium hydrogen conversion rate while maintaining the ferrite in its solid phase [26].[15] Each step has been demonstrated, but investigation of reaction kinetics and materials cyclability are ongoing.

Table 3-12: Summary of ferrite cycle chemistry

Stage	Net Reaction	Notes/Comments
Reduction	$NiFe_2O_4 + 0.67\ ZrO_2 \rightarrow MeO + 0.5x\ O_2 + 0.67\ ZrO_2$	Endothermic reduction of nickel ferrite at 1,450 C
Oxidation	$MeO + xH_2O + 0.67\ ZrO_2 \rightarrow NiFe_2O_4 + 0.67\ ZrO_2 + xH_2$	Exothermic oxidation of metal oxide at 1,000 C

3.4.2 Plant Design

The ferrite cycle directly uses concentrated solar power to provide thermal energy to a single integrated thermal receiver / chemical reactor to produce hydrogen. Due to the high reaction temperatures (well over 1,000 C), thermal storage is not practical for this system, so it operates only "on-sun". With the exception of a small amount of electricity to power auxiliaries, the ferrite cycle is entirely thermally driven.

The solar field for the ferrite plant was designed using SolTrace, a spreadsheet-based solar field design tool [27,28]. To meet the high temperature requirement of the ferrite reduction reaction, the solar field design uses an arrangement of three heliostat fields and secondary concentrators per tower Figure 3-11. Key solar field design parameters are summarized in Table 3-13.

[15] At temperatures over 1,525 C, ferrite forms a liquid slag

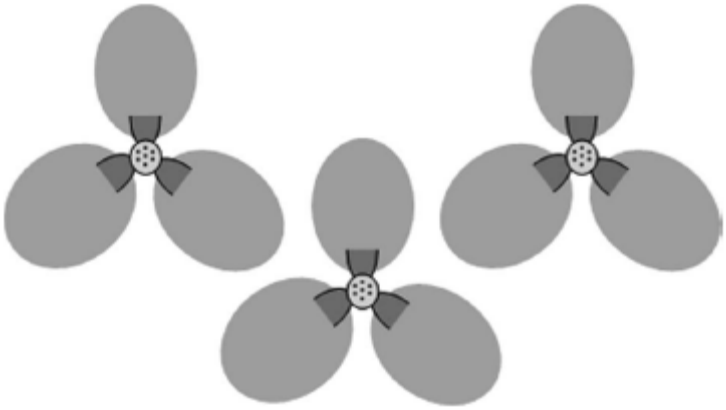

Figure 3-11: Schematic of ferrite solar field layout (not to scale) [29]

Table 3-13: Summary of ferrite solar plant operational characteristics

Parameter	2015	2025
Design point (TPD H_2)	100	100
Heliostat area (m^2)	2,090,000	2,090,000
Secondary concentrator area (m^2)	2,662	2,662
Tower height (m)	223	223
Number of towers	6	6
Number of solar fields	3 per tower	3 per tower
Secondary concentration	3,868 Suns	3,868 Suns
Solar-to-heat efficiency (annual avg)[16]	40%	40%
Solar auxiliaries	0.4 MW_e	0.4 MW_e
Thermal Storage	None	None
Max temperature	1,450	1,450
Receiver (avg)	Approx 200 MW	Approx 200 MW

The process flowsheet for the ferrite cycle was developed using a combination of FactSage and Aspen Plus analysis. The ferrite production plant is implemented as a single integrated thermal receiver/reactor chamber, which includes an insulated absorbing cavity filled with a series of parallel tube bundles (Figure 3-12). The inside of each tube contains high-surface area (100 m^2/g) and highly porous zirconium oxide (ZrO_2) substrate coated with a thin film of ferrite [26].

Each tube alternates between the oxidation reaction and the reduction reaction using the following operational concept:

1. During the reduction reaction, tubes are heated to approximately 1,450 C, where oxygen is evolved and the surface of the thin-film ferrite is reduced to metal oxide.
2. As oxygen is evolved, it is removed from the reactor chamber using a vacuum pump.
3. Following reduction of ferrite to metal oxide, the chemical cycle is completed by pumping steam into the evacuated tube. The oxidation reaction converts the metal oxide back to ferrite and evolves hydrogen in the process. This reaction occurs at lower temperature than the reduction reaction – approximately 1,000 C.

[16] See section 2.3 for definition of solar-to-heat efficiency

4. Heat recovered from the metal oxide is used to preheat the ferrite for the next reduction reaction. Heat recovered from the hydrogen product and oxygen by-product is used to preheat the incoming water/steam for the oxidation reaction.

A diagram of the ferrite process flowsheet is shown in Figure 3-13. Note that although the flowsheet depicts the unit processes as discrete reactors, as conceived, the process is implemented in a single reactor vessel [31]. Hydrogen is produced continuously through a series of solenoid valves and tubes switching between redox cycles – half of the tubes always undergoing reduction and half always undergoing oxidation.

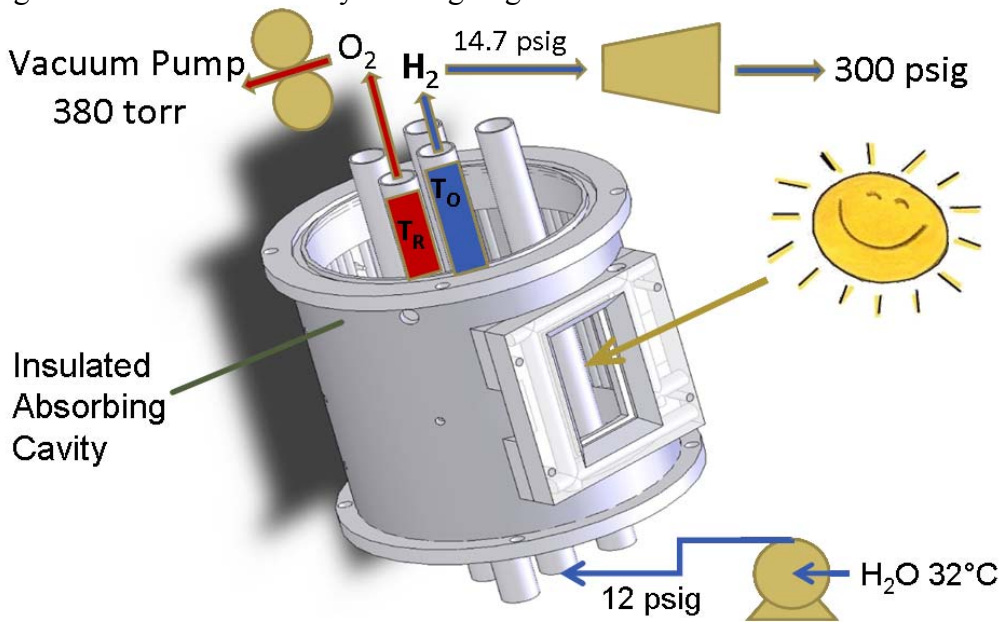

Figure 3-12: Ferrite reactor concept [30]

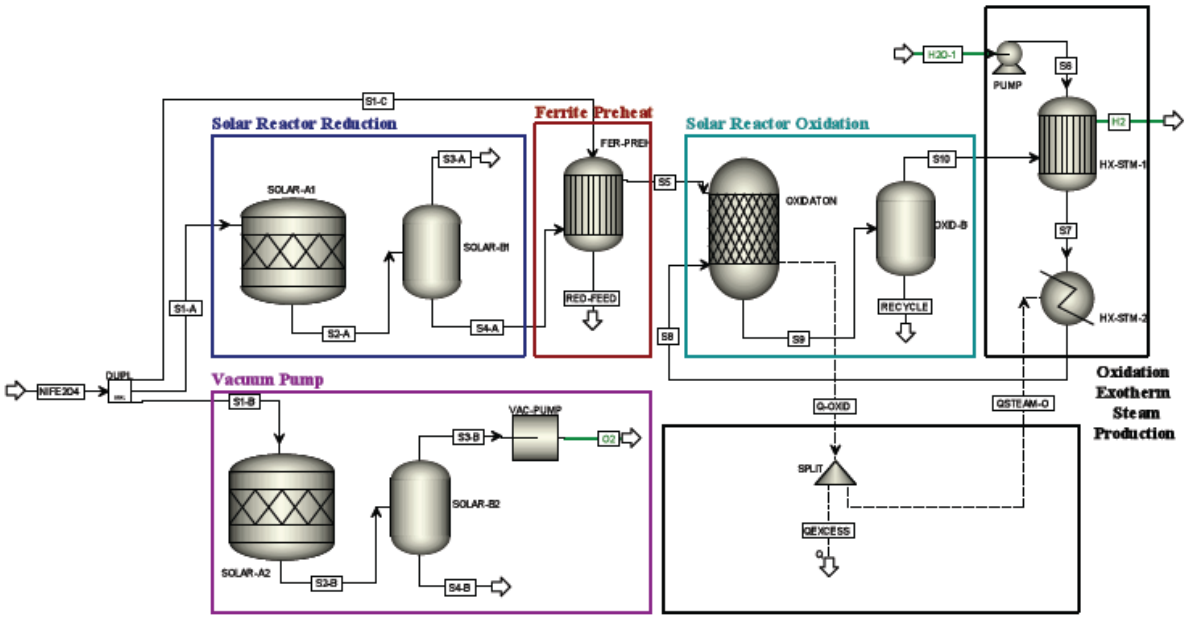

Figure 3-13: Ferrite process flowsheet

The plant is designed to produce an average of 100 TPD of hydrogen, but the rate of hydrogen production is continuously adjusted throughout the day and year by matching the reaction's cycle time to the available solar thermal energy. A summary of the key ferrite chemical process operational characteristics is included in Table 3-14.

Table 3-14: Summary of Thin Film Ferrite chemical plant operational characteristics

Parameter	2015	2025
Design point (TPD)	100	100
Max temperature	1,450 C	1,450 C
# of reactions	2	2
Oxidation/Reduction Reactor	6 Multi-tube reactor/receivers	6 Multi-tube reactor/receivers
Duty cycle (hrs per day)	Approx 8 hrs/day	Approx 8 hrs/day
Cycle time (min)	5 min	1 min
Thermal energy use	64 kWh/kg H_2	64 kWh/kg H_2
Auxiliaries Electricity use	1.1 kWh/kg H_2	1.1 kWh/kg H_2
Electricity generated	-2.8 kWh/kg H_2	-2.8 kWh/kg H_2
Net Electricity	-1.7 kWh/kg H_2	-1.7 kWh/kg H_2
# of laborers (solar + chem)	45	45
STCH efficiency[17]	52%	52%

While the basic cycle chemistry of the nickel ferrite cycle is fairly well understood and the basic plant concept has been defined, several aspects of the ferrite STCH cycle are currently unproven and under investigation:

- **Reaction rate:** The rate of the ferrite oxidation reaction is influenced by the surface area and the heat transfer properties of the ferrite thin-film within the oxidation reactor tubes. The ferrite analysis is based on a 5 nm nickel ferrite film deposited on a 100 m^2/g ZrO_2 support. The current analysis assumes that the reaction proceeds to thermodynamic equilibrium within a defined average cycle time that is anticipated to improve over time (5 minutes for the 2015 system, 1 minute for the 2025 system).[18] Currently, cycle times on the order of 15 minutes have been demonstrated. It should also be noted that a fully optimized ferrite STCH process would select the residence time to maximize the integrated hydrogen production rate rather than allow it to proceed to chemical equilibrium, as is currently assumed. However, the analysis has not yet proceeded to this level of refinement.
- **Ferrite thin film durability:** While ferrite thin films have demonstrated property retention over limited durability testing (on the order of 50 cycles), no testing has yet been performed on their resilience over the more than 100,000 cycles per year that could be seen in an operational plant. The current analysis implicitly assumes that 6% of the ferrite and substrate are replaced each year.
- **Reactor design:** The reactor design is still in the conceptual design phase – i.e., such a system has not been built and tested, but work is progressing for an on-sun demonstration. A viable system will require materials that are resilient to the high reaction temperatures and the thermal cycling seen during normal operation. In addition, the recuperation concept seems theoretically sound, but may be challenging to implement. The current analysis assumes that the reactor is composed of silica carbide tubes, on which thermal fatigue analysis is ongoing. It is also assumed that 79% of the heat is recovered, which may be challenging in practice.

[17] See section 2.3 for definition of heat-to-hydrogen efficiency
[18] Note that under operational conditions, these cycle times would vary to adjust to the solar heat input

- **Ferrite cost:** Thin film nickel ferrite is not currently commercially available, so obtaining accurate high-volume cost estimates is problematic. Ferrite costs were estimated by adding a markup to the cost of the constituent elements, ferrocene and nickelocene.

3.4.3 Capital & Operating Costs

Capital costs for the ferrite cycle chemical plant were developed using equipment sizing calculations derived from the FactSage and Aspen Plus analysis, and a combination of vendor quotes and capital cost estimation databases for major chemical plant capital costs. A summary of the plant capital and operating costs is shown in Table 3-15. The major cost contributors are the heliostat field and the integrated receiver/reactor. As shown, the primary operating costs are associated with equipment maintenance and materials replacement (assumed 6% per year for the chemicals and chemical plant equipment). Because the plant generates its own electricity using heat recovered from the reduction reaction, the net variable operating costs are relatively low.

Table 3-15: Ferrite STCH cycle capital and operating costs

Category	2015	2025	Comments
Solar Plant Installed Capital Costs			
Heliostats	$264	$188	$127.5/$m^2$ (2015), $90/$m^2$ (2025) [6]
Secondary Concentrators	$0.6	$0.6	Assumes 10X heliostat cost [26]
Towers	$63	$63	6 223 m tower, scaled from [4]
Controls	-	-	
Balance of Plant	-	-	
Total Solar Cost	**$328**	**$252**	**Sum of the above**
Chemical Plant Installed Capital Costs			
Solar Reactor	$123	$25	Bottom-up estimate based on vendor quote for SiC tubes with a jacketed pressure vessel shell (6 reactors total) [48,49]
Compressors	$32	$32	3 stage compressor, from DOE components model
Vacuum Pumps	$14	$14	3 cast iron blowers per reactor (matche.com) [48]
Water Pumps	$0.3	$0.3	2 per reactor (matche.com) [48]
Turbine	$1.2	$1.2	One 2.3 MW_e turbine, from CAPCOST [24]
Heat Exchangers	$1.0	$1.0	Shell & Tube heat exchanger, one per tower [48]
ZrO_2	$0.1	$0.01	USGS material cost
Ferrite	$71	$14	Ferrite ~ $270/kg ($225/kg for precursors + 20% markup); 5 min per cycle (2015 case) / 1 min per cycle (2025 case)
Chemical Plant Cost	**$242**	**$88**	Sum of the above
Chemical Plant Installed Capital Costs			
Total Direct Capital	$570	$339	Sum of chemical & solar plant cost
Indirect Capital	$183	$122	Includes contingency, fees, engineering & design, site preparation, and land cost
Total Capital Cost	**$753**	**$461**	Sum of indirect & direct capital
Annual Operating Cost			
Fixed op costs	$28	$15	Includes labor, prop taxes, insurance, maintenance & repairs.
Variable op costs	$0.1	$0.1	Includes electricity & water
Total Operating Cost	**$28**	**$15**	**Sum of fixed and variable operating costs**

3.4.4 Results

The results of the ferrite cycle cost analysis are shown in Table 3-16.

Table 3-16: Ferrite Cycle Results

Analysis Year	Capital	Fixed O&M	Var O&M	Total	Critical Assumptions
2015	$3.27	$0.79	$0.00	**$4.06**	- 5 minute cycle time - 15 year ferrite and substrate lifetime - Ferrite cost = $270/kg - Reactor design & heat integration
2025	$2.01	$0.41	$0.00	**$2.42**	- 1 minute cycle time - 15 year ferrite and substrate lifetime - Ferrite cost = $270/kg - Reactor design & heat integration

Single variable sensitivity analysis was conducted on the ferrite process for several critical parameters (Figure 3-14 and Figure 3-15). The results indicate that the ferrite cycle time is the dominant cost driver for the process, although the required materials replacement rate is also important – and becomes more important if the cycle time is slower (and hence more ferrite is required.)

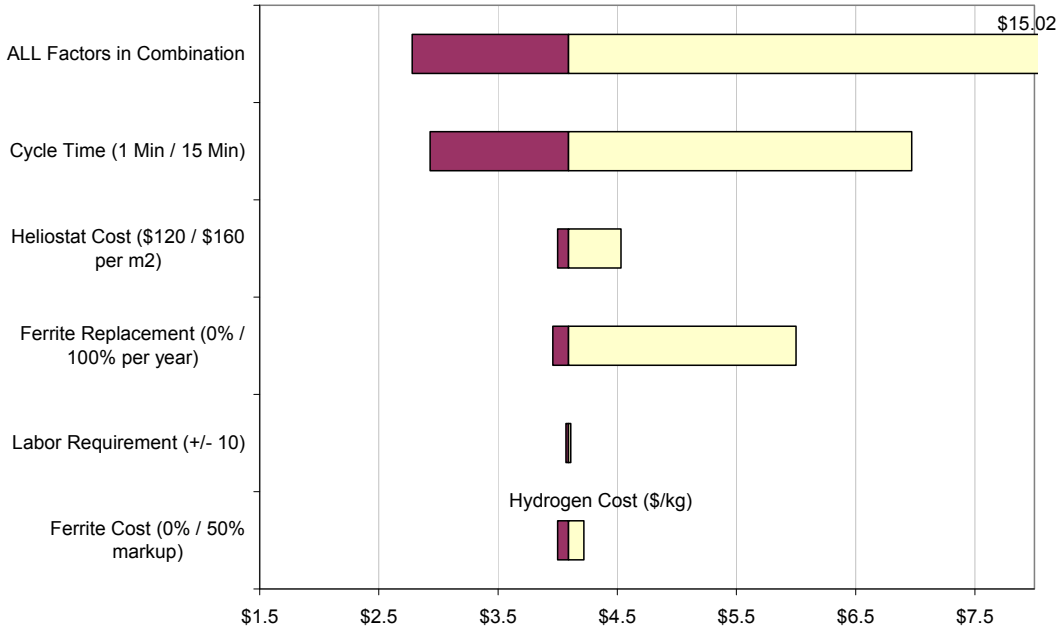

Figure 3-14: Ferrite Cycle 2015 Single Variable Sensitivity

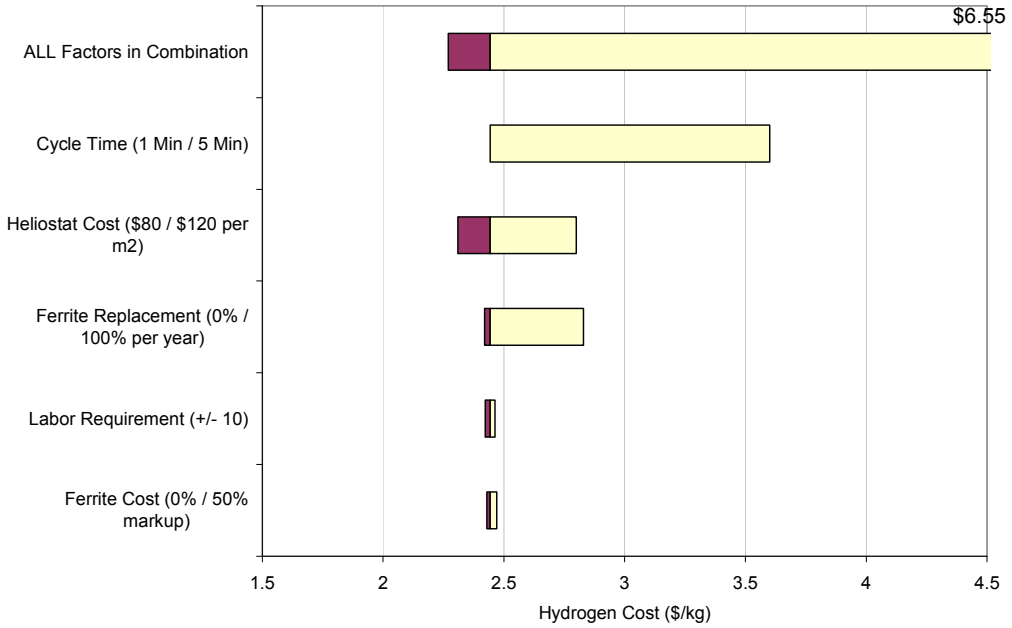

Figure 3-15: Ferrite Cycle 2025 Single Variable Sensitivity

3.5 Sulfur Ammonia (S-A) STCH Process

3.5.1 Overview

Analysis of the sulfur-ammonia (SA) water splitting cycle was conducted by SAIC. Research on this cycle is still ongoing. As such, the results presented in this section do not reflect a fully validated or optimized chemical process or plant design. They reflect a preliminary evaluation of the process economics using an approach and basic assumptions that are consistent with the approach used by other STCH research teams.

The sulfur-ammonia cycle is a three step chemical process, summarized in Table 3-17. It is a modification of the Bowman-Westinghouse hybrid sulfur cycle discussed in section 3.2. One of the issues with the hybrid-sulfur cycle is the energy intensive separation and concentration of sulfuric acid. The sulfur-ammonia cycle addresses this issue by using ammonium sulfite, a highly water soluble salt, to form the electrolyte, thereby simplifying the hydrogen production step [32].

There are three primary chemical reactions: the electrolysis of ammonium sulfite to ammonium sulfate (which produces hydrogen), the thermal decomposition of ammonium, and the thermal decomposition of sulfur trioxide (which liberates oxygen). The products of ammonum sulfate decomposition are three gasses, ammonia, water and sulfur trioxide. The sulfur trioxide is stripped from the gas mixture using a molten salt mixture containing alkali sulfate. The adsorption of the sulfur trioxide can be formally represented as a chemical reaction forming pyrosulfate from sulfate. Sulfur trioxide desorption from the melt reverses the adsorption process. Finally, the product gasses from the chemical reaction steps condense to form the ammonium sulfite required for the electrolysis step. The condensation step can also be formally represented as a chemical reaction.

Table 3-17: Sulfur-Ammonia Cycle Reaction Summary

Stage	Net Reaction	Notes/Comments
H_2 production	R1. $(NH_4)_2SO_{3\,(aq)} + H_2O_{(l)} \rightarrow H_{2\,(g)} + (NH_4)_2SO_{4\,(aq)}$	Electrolysis at 130 C
Salt decomposition	R2. $(NH_4)_2SO_{4\,(aq)} \rightarrow 2NH_{3\,(g)} + SO_{3\,(g)} + H_2O_{(g)}$	Solar thermal at 400 C
Oxygen evolution	R3. $SO_{3\,(g)} \rightarrow SO_{2\,(g)} + 0.5O_{2\,(g)}$	Solar thermal at 850 C
SO_3 absorption	S1. $SO_{3\,(g)} + K_2SO_{4\,(l)} \rightarrow K_2S_2O_{7\,(l)}$	Spontaneous at 400 C
SO_3 desorption	S2. $K_2S_2O_{7\,(l)} \rightarrow K_2SO_{4\,(l)} + SO_{3\,(g)}$	Solar thermal at 550 C
Condensation	S3. $SO_{2\,(g)} + 2NH_{3\,(g)} + H_2O_{(l)} \rightarrow (NH_4)_2SO_{3\,(aq)}$	Spontaneous below 300 C

3.5.2 Plant Design

The sulfur-ammonia chemical plant process was modeled using ASPEN Plus, but the simulation described will be updated as the overall process is optimized. The final version may operate at higher temperatures, and employ the alternate options for thermal storage that are currently being explored. The current ASPEN flowsheet generates a large amount of excess electricity because excess waste heat is available at high temperature when SO_3 is decomposed using solar heat. This could be beneficial if the financial calculations allow credit for electricity sold to the grid, which had been the case during a prior revision of the DOE guidelines. However, the current guidelines do not allow for this credit. For the 2025 case, SAIC has assumed that process

optimizations reduce the thermal requirement by 15%, and that the process will not deliver excess electricity to the grid. This assumption has yet to be validated using ASPEN Plus.

The process utilizes solar thermal energy to drive the oxygen evolution (Steps R2, R3, and S2 in Table 3-17), which occur at 350 C to approximately 850 C. Solar thermal energy is collected and stored from heliostat fields using either a falling sand or a molten salt receiver mounted on a solar power tower. The selection will depend on what is feasible given the actual temperatures of reaction. A small thermal storage buffer (on the order of 2 hours) is used to reduce transients.

The energy requirement for the electrolytic reaction (Step R1) is supplied by power generated onsite via a power recovery turbine. The chemical absorption stage proceeds spontaneously at relatively low temperature. Approximately 90% of the energy is sourced from solar thermal energy, and 10% from electricity under the electric heating scenario. Heat recovered from the various reactant streams is used to preheat reactants for the oxygen evolution reactions, and to drive a power recovery turbine that helps power the plant operations. In general, the S-A process consists of liquid/gas reactions, so separations are straightforward.

The solar field is a scaled version of that used for the 2015 hybrid-sulfur analysis.[19] The key solar field design parameters for the Sulfur-Ammonia process are summarized in Table 3-18. The chemical plant parameters are summarized in Table 3-19. Compared to the 2015 system, the 2025 chemical plant assumes a 15% reduction in the thermal energy requirement (due to assumed improvements in heat integration), and assumes that the electrolyzer efficiency and power density improves. Electrolyzer performance has been demonstrated at approximately 0.7 V and 100 mA/cm^2 for relatively short durations [33]. The 2015 system is based on this condition, while the 2025 system assumes the current density increases while the voltage drops.

Table 3-18: Summary of Sulfur-Ammonia solar plant operational characteristics

Parameter	2015	2025
Design point (TPD H_2)	100	100
Heliostat area	3,911,000 m^2	3,325,000 m^2
Tower height	230 m	230 m
Number of towers	5	5
Number of solar fields	1 per tower	1 per tower
Solar field efficiency	46%	46%
Solar auxiliaries (Daytime only)	0.9 kWh/kg H_2	0.8 kWh/kg H_2
Thermal Storage	1,500 MWh_{th}	1,280 MWh_{th}
Max temperature	~900 C	~900 C
Receiver (peak)	811 MW_{th} per receiver	860 MW_{th} per receiver

[19] Initially, SAIC had used an internally developed field optimization tool for the solar field design. However, the resulting plant design appeared to by inconsistent with the other analyses, so the hybrid sulfur field design was adapted for this case study.

Table 3-19: Summary of SA chemical plant operational characteristics

Parameter	2015	2025
Design point (TPD H_2)	133	133
Max temperature	~850 C	~850 C
# of reactions	5	5
Duty cycle (hrs per day)	8-12 hrs – other 24 hrs - electrolysis	8-12 hrs – other 24 hrs – electrolysis
Thermal energy	138 kWh/kg H_2	116 kWh/kg H_2
Electrolyzer energy	16 kWh/kg H_2	12.8 kWh/kg H_2
Auxiliary energy	2.0 kWh/kg H_2	2.0 kWh/kg H_2
Electricity Generated	-21 kWh/kg H_2	-15.6 kWh/kg H_2
Net Electricity Use	-	-
Electrolyzer Design Pt	0.7 V, 100 mA/cm^2	0.4 V, 500 mA/cm^2
Electrolyzer Refurbishment	5 yrs	10 yrs
# of laborers (solar + chem)	76	76
STCH efficiency[20]	24%	29%

3.5.3 Capital and Operating Costs

The major capital equipment includes the electrolysis system, reactor vessels for the three intermediate oxygen evolution reactions, mixing tanks (for chemical adsorption and reactant recycle flows), and heat integration (cooling towers and heat exchangers). With the exception of the electrolysis system, the major capital equipment for the S-A plant consists of commonly-used, commercially available items. Even the electrolysis system is not far removed from the Chlor-Alkali process used for commercial production of chlorine and sodium hydroxide. While the corrosive properties of reactants (ammonia, SO_3, SO_2) warrant stainless steel, major materials of construction issues are not anticipated.

Major capital and operating costs are summarized in Table 3-20. Due to its relatively low efficiency, the S-A cycle requires a large heliostat field, as well as associated towers, receivers, and thermal storage, which collectively constitute the bulk of the capital cost. The key cost driver for the chemical plant is the electrolysis reactor. Major operating costs include general maintenance and repairs.

[20] See section 2.3 for definition of solar-to-heat efficiency

Table 3-20: S-A STCH cycle capital and operating costs

Category	2015	2025	Comments
Solar Plant Installed Capital Costs			
Heliostats	$554	$335	$127.5/$m^2$ (2015), $90/$m^2$ (2025) [6]
Receivers	$209	$45	2015: 5 x 890 MW_{th} molten salt receivers [4] 2025: 4 x 890 MW_{th} falling sand receivers [6]
Towers/Piping	$56	$44	4 (2015) / 5 (2025) 223m towers [4]
Thermal Storage	$34	$29	$20/$kWh_{th}$ [17,18,19]; 1,500 (2015) / 1,280 MWh_{th}
Controls	$2	$2	[4]
Balance of Plant	$33	$34	Scaled from [4]
Total Solar Cost	**$889**	**$490**	**Sum of the above**
Chemical Plant Installed Capital Costs			
Electrolyzer System	$66	$17	Active area = 76,000 m^2 (2015), 23,000 m^2 (2025); $720/$m^2$ (2015), $640/$m^2$ (2025) x 1.2X installation factor. See App C.[21]
Initial Chemical Cost	$20	$20	NH_3SO_4 ($191/mT), K_2SO_4 and $K_2S_2O_7$ ($200/mT)
Compressors	$19	$19	[24]
Heat Exchangers	$5	$5	[24]
Pumps	$0.5	$0.5	[24]
Turbine	$12	$12	Based on power block from [4]
Reactors	$7	$7	[24]
Mixers & Tanks	$7	$7	[24]
Cooling Towers	$62	$62	[24]
Furnace/High temp reactor	$0	$0	No cost included
Chemical Plant Cost	**$213**	**$164**	Sum of the above
Chemical Plant Installed Capital Costs			
Total Direct Capital	$1,101	$654	Sum of chemical & solar plant cost
Indirect Capital	$399	$236	Includes contingency, fees, engineering & design, site preparation, and land cost
Total Capital Cost	**$1,500**	**$890**	Sum of indirect & direct capital
Annual Operating Cost			
Fixed op costs	$37	$27	Includes labor, prop taxes, insurance, maintenance & repairs.
Variable op costs	$-	$-	Includes water
Total Operating Cost	**$37**	**$27**	**Sum of fixed and variable operating costs**

3.5.4 Results

A summary of the hydrogen cost projected by the S-A H2A analysis is shown in Table 3-21. As shown, the projected cost for both the 2015 and 2025 case exceeds the DOE near-term target of $5 to $6 per kg and the long-term target of $2 to $3 per kg by a wide margin. As discussed previously, the state of the S-A analysis is less mature relative to several of the other systems characterized in this report. Several factors contribute to the high projected cost of the S-A system, and it remains an open question as to what extent these factors reflect fundamental

[21] Some components of the electrolysis reactor balance of plant are included elsewhere in the cost estimates.

challenges to the process, and to what extent they reflect the relative immaturity of the ongoing research effort.

The process efficiency projected based on the current analysis is lower than that of the other cycles that have been examined (24 to 28%, as compared to 30 to >50%). However, the process is not fully developed and is not optimized at present. As development proceeds, there may be opportunities for further improving the cycle efficiency.

Table 3-21: S-A Hydrogen Cost Breakdown

Analysis Year	Capital	Fixed O&M	Var O&M	Total	Critical Assumptions
2015	$6.71	$1.03	$0.00	**$7.74**	- Heliostat cost of $127/m^2 - Electrolyzer: 0.7 V, 100 mA/cm^2 - Electrolyzer cost of $720/m^2 uninstalled - 5 yr electrolysis reactor lifetime
2025	$3.89	$0.76	$0.00	**$4.65**	- Heliostat cost of $90/m^2 - Electrolyzer: 0.4 V, 500 mA/cm^2 - Electrolyzer cost of $640/m^2 uninstalled - 10 yr electrolysis reactor lifetime - Thermal energy reduced by 15%

3.6 Zinc Oxide (ZnO) STCH Process

3.6.1 Overview

The zinc oxide cycle analysis presented was conducted by the University of Colorado research team. The zinc oxide (ZnO) cycle (Table 3-22) is a two-step water splitting process. The first step is the reduction of solid ZnO powder into zinc metal and oxygen. The temperature required for the dissociation of ZnO is 1,700 to 1,800 C. Experimental results have shown that the kinetics of the metal reduction stage are most favorable for small particles of ZnO dispersed in an inert carrier gas, and have demonstrated forward reaction yields of 60%. However, a maximum overall conversion of 18% has been demonstrated. This is due to a strong tendency for the dissociated Zn and oxygen to recombine into ZnO at high temperature. To achieve high conversion rates, it is necessary to rapidly cool the reaction products. The second step entails hydrolysis of zinc metal at 400 C, during which hydrogen is evolved and the ZnO regenerated. This reaction has demonstrated 100% yields of hydrogen, but requires long residence times [34].

Table 3-22: Zinc Oxide Cycle Reaction Summary

Stage	Net Reaction	Notes/Comments
Metal Reduction	$ZnO \rightarrow Zn + 0.5O_2$	Reduction of ZnO at 1,750 C; back reaction presents a major challenge
Hydrolysis	$Zn + H_2O \rightarrow ZnO + H_2$	Hydrolysis of zinc, occurs at 400 C; slow kinetics

3.6.2 Plant Design

The ZnO plant uses solar thermal energy to drive the dissociation of ZnO. Residual heat from this reaction provides the thermal energy for the hydrolysis step. Electricity is used to drive solar and plant auxiliaries – notably the separation of argon from the oxygen product following the ZnO dissociation reaction. A portion of this electricity requirement is generated internally from a power recovery turbine.

The dissociation reaction occurs in a thermal receiver located on top of a solar power tower. Solar thermal energy is concentrated on the receiver from surrounding heliostat fields using secondary concentrators, which provide the solar flux needed to achieve the high operating temperature. The dissociation reaction occurs on-sun during daylight hours, but the zinc generated as a result is stored in insulated tanks at high temperature, which enables the hydrolysis step to proceed 24 hours per day. An illustrative diagram of the heliostat field layout is shown in Figure 3-16. Critical solar plant design characteristics are summarized in Table 3-23.

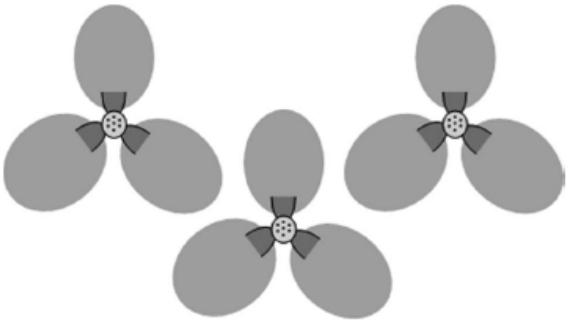

Figure 3-16: Illustrative ZnO heliostat field layout [29]

Table 3-23: Summary of ZnO solar plant operational characteristics

Parameter	2015	2025
Design point (TPD H_2)	100	100
Heliostat area (m^2)	2,517,000 m^2	2,349,000 m^2
Secondary concentrators (m^2)	4,800 m^2	4,500 m^2
Secondary concentration	7,414 suns	7,414 suns
Tower height (m)	250	250
Number of towers	15	14
Number of solar fields	3 per tower	3 per tower
Solar field efficiency	45%	45%
Solar auxiliaries (MW_e)	0[22]	0
Thermal Storage	13 hr ZnO storage (2,500 MT)	13 hr ZnO storage (2,500 MT)
Max temperature	1,800 C	1,800 C
Receiver (MW_{Th}, peak)	112 MW_{th} (each)	112 MW_{th} (each)

The ZnO chemical process was modeled using Aspen. A simplified diagram of the resulting flowsheet is shown in Figure 3-17. As conceived, for the 2015 case, the high-temperature ZnO reduction reaction would occur in a fluid-wall multi-tube reactor composed of a siliconized graphite outer receiver cavity surrounding two concentric graphite tubes. The outer graphite tube acts as a heating tube, while the reaction occurs within the inner tube. The reactor is designed such that the flowing reactant gases within the reaction tube form a fluid wall, thereby preventing unwanted side reactions. The 2025 case uses a similar concept, but with a single siliconized graphite tube. This has the benefit of reducing the quantity of carrier gas, thereby simplifying downstream portions of the cycle [35]. Prior to entering the reactor, solid ZnO is preheated by the reactor product[23] and dispersed in an argon gas carrier. At the reactor outlet, the products are quenched from 1,750 C to approximately 900 C to minimize recombination. The quench process has not yet been fully specified, but it is assumed that no heat is recovered during quench. The gaseous product stream passes through a solid filtration system (to remove Zn metal) and then a vacuum stream adsorber (VSA), which separates argon gas for recycling. The Zn metal product is then stored at high temperature for subsequent use in the hydrolysis reaction. A Zn to ZnO conversion rate of 70% (2015) and 85% is assumed for the reduction reaction [34, 36].

[22] The ZnO economic analysis does not appear to account for electricity to drive the solar plant auxiliaries
[23] Heat is recovered after the quench process.

Figure 3-17: ZnO chemical plant process flowsheet [34]

The hydrolysis reaction occurs in a fluidized bed reactor at 400 C, and is implemented as a batch process with a 30 minute residence time. Heat recovered from this process is used to drive a power recovery turbine, which is then used to drive plant auxiliaries. The hydrolysis reaction is assumed to achieve 100% hydrogen conversion.

The ZnO plant is implemented with one decomposition reactor per tower, and a single centralized hydrolysis reactor module. The hydrolysis reactor module would consist of the reactor itself, the power recovery block, and storage tanks. However, it is not clear from the information provided whether the tertiary decomposition equipment – i.e., preheaters, filtration, and the VSA separation unit – is implemented as one per tower, or as a single centralized system. It is also not clear how solids are transported throughout the plant.

A summary of the ZnO chemical plant operational characteristics is shown in Table 3-24. The 2025 plant includes a number of assumed design enhancements compared to the 2015 case: (1) The 2025 case assumes a higher Zn/ZnO conversion efficiency, which reduces the overall thermal requirement, but increases the reactor size (to account for the longer residence time); (2) The 2025 specification is based on a modified decomposition reactor, which reduces the amount of Argon and simplifies the VSA separation; (3) In the 2025 case, the hydrolysis reaction occurs at pipeline high pressure (as opposed to atmospheric), obviating the need for a separate hydrogen compression step.

Table 3-24: Summary of ZnO chemical plant operational characteristics

Parameter	2015	2025
Design point (TPD)	133	133
Max temperature	1,750	1,750
# of reactions	2	2
ZnO Decomposition Reactor	15 fluid wall, multi-tube reactors	14 single tube reactors
Hydrolysis Reactor	1 fluidized bed batch reactor, 1bar	1 fluidized bed batch reactor, 20 bar
Duty cycle	8 hrs – reduction reaction 24 hrs – hydrolysis reaction	8 hrs – reduction reaction 24 hrs – hydrolysis reaction
Zn/ZnO Conversion η	70%	85%
Argon separation	3-stage VSA	Single stage VSA
Thermal energy use[24]	83 kWh/kg H_2	80 kWh/kg H_2
VSA electricity use	7 kWh/kg H_2	2.0 kWh/kg H_2
Auxiliaries electricity use	0.5 kWh/kg H_2	0.5 kWh/kg H_2
Energy generated	-2.8 kWh/kg H_2	-2.8 kWh/kg H_2
Net electricity use	4.7 kWh/kg H_2	-[25]
# of laborers (solar + chem)	80	77
STCH efficiency[26]	35%	42%

3.6.3 Capital and Operating Costs

A summary of the ZnO capital and operating costs is shown in Table 3-25. The chemical plant equipment costs were estimated using a combination of vendor quotes, data from Peters & Timmerhaus, and bottom-up cost methodology. Because the ZnO analysis was completed in 2008, it was necessary to modify the information provided by the University of Colorado to reflect updates in the baseline financial and operational assumptions. These modifications included updating the capital and operating costs to 2007$ and adjusting several assumptions used to calculate the indirect capital costs. While the ZnO analysis was largely completed and validated by TIAX prior to its down-selection, there were several outstanding questions which are detailed below Table 3-25. We do not anticipate that these issues will materially affect the final results.

The primary cost drivers for the ZnO cycle are the heliostat field and solar power towers. The key elements of the ZnO chemical plant include the decomposition reactors (one per tower) and the vacuum swing adsorber used for recycling the argon feed.

[24] Average thermal power to the receiver/reactor on a 24 hour basis

[25] As specified, the 2025 ZnO plant is a net producer of a small amount of electricity (1.2 MW_e). However, more recent guidelines specify that no by-product electricity generation credit is allowed. In addition, as discussed in the capital & operating costs section, it is not clear that the ZnO plants adequately account for solar or chemical plant auxiliaries. As such, the net production is estimated to be 0.

[26] See section 2.3 for definition of solar-to-heat efficiency

Table 3-25: ZnO STCH cycle capital and operating costs

Category	2015	2025	Comments
Solar Plant Installed Capital Costs			
Heliostats	$318	$211	$127.5/m^2 (2015), $90/m^2 (2025) [6]
Tower	$243	$227	14 (2015) / 15 (2025) 250 m towers [4]
Secondary Concentrator	$18	$14	10X heliostat cost
Receiver	$66	$60	Based on vendor quotes for graphite tubes; does not include housing
Controls	-	-	
Balance of Plant	-	-	
Total Solar Cost	**$655**	**$512**	**Sum of the above**
Chemical Plant Installed Capital Costs			
Preheater/Recovery Heater	$17	$17	[37]
Bag Filters/Tanks	$2	$2	Solid filtration and insulated storage [37]
Zinc oxide	$4	$4	2,500 tons (13 hr supply), $1850/tonne
Steam Generation	$7	$7	[37]
Hydrolysis reactor	$2	$2	Fluidized bed batch reactor, 30 min residence time, 20 bar stainless (2025) or glass-lined 1 bar [37]
Pumps/motors	$10	$2	[37]
VSA and Screw Compressors	$76	$25	Vendor quote for 3 stage (2015), 1 stage (2025)
Power Recovery Turbine	$5	$5	11.5 MW_e turbine, $450/$kW_e$ installed [37]
H2 Compression	$28	-	From H_2 Components Model
Argon	-	-	Not included
Solids Conveying	-	-	Not included
Chemical Plant Cost	**$152**	**$65**	Sum of the above
Chemical Plant Installed Capital Costs			
Total Direct Capital	$807	$576	Sum of chemical & solar plant cost
Indirect Capital	$290	$218	Includes contingency, fees, engineering & design, site preparation, and land cost
Total Capital Cost	**1,097**	**$794**	Sum of indirect & direct capital
Annual Operating Cost			
Fixed op costs	$32	$24	Includes labor, prop taxes, insurance, maintenance & repairs.
Variable op costs	$15	$0.4	Net electricity & water
Total Operating Cost	**$47**	**$25**	**Sum of fixed and variable operating costs**

Outstanding Questions:

Plant layout and materials transport: Specific details regarding the plant design were not clear from the information provided. In particular, it is not clear how solids are transported (no means of conveyance is included in the cost analysis) and it is not clear whether the VSA and pre-heater are implemented as single centralized units, or as individual modules coupled to each decomposition reactor. If the preheat occurs at a centralized location, there may be additional thermal losses that are not accounted for.

Argon supply: The cost analysis does not account for initial or replacement costs for the argon carrier, which could add on the order of $18M to the initial cost.[27]

[27] Based on 3:1 molar ratio of Ar to ZnO, and Argon cost of $5,000 per tonne

Electricity generation: Auxiliary electricity use may be understated for both the 2015 and 2025 case. The primary electricity consumer is the VSA system, which is explicitly accounted for in the analysis. The 2015 case includes 2.1 MW_e for all other chemical and solar plant consumers, and the 2025 case includes 0.7 MW_e for the other consumers. These numbers are significantly lower than those seen for other plants, which might typically include 5 to 10 MW_e for solar and chemical plant auxiliaries.

Reactor Cost: The reactor cost estimates appears to only account for the cost of tubes, plus an installation cost factor. It does not include the cost for housing.

3.6.4 Results

A summary of the hydrogen cost projected by the zinc oxide H2A analysis is shown in Table 3-26. As shown, the 2015 case is close to the near-term target of $5 to $6 per kg, while the 2025 case is approximately 40% higher than the long-term target of $2 to $3 per kg. The major contributor to the hydrogen selling price is the plant capital cost (approximately 80% of the total). As shown in Table 3-25, the bulk of the direct capital expense consists of the solar plant, for which the heliostats and towers are the primary cost driver.

Table 3-26: Zinc Oxide Cycle Hydrogen Cost Breakdown

Analysis Year	Capital	Fixed O&M	Var O&M	Total	Critical Assumptions
2015	$4.83	$0.96	$0.28	**$6.07**	- 70% Zn/ZnO Conversion (no back reactions) - Reactor durability - $127/m^2 heliostat cost
2025	$3.50	$0.67	$0.01	**$4.18**	- 85% Zn/ZnO Conversion (no back reactions and improved yields) - Reactor durability - Reactor modifications (reduces argon supply, VSA cost, electricity use) - $90/m^2 heliostat cost

The results of the single-variable sensitivity analysis for the 2015 and 2025 cases are shown in Figure 3-18 and Figure 3-19. For the 2025 case, using the alternate economic assumptions is the only single variable that can achieve the $3/kg target, although several factors in combination could also do so.

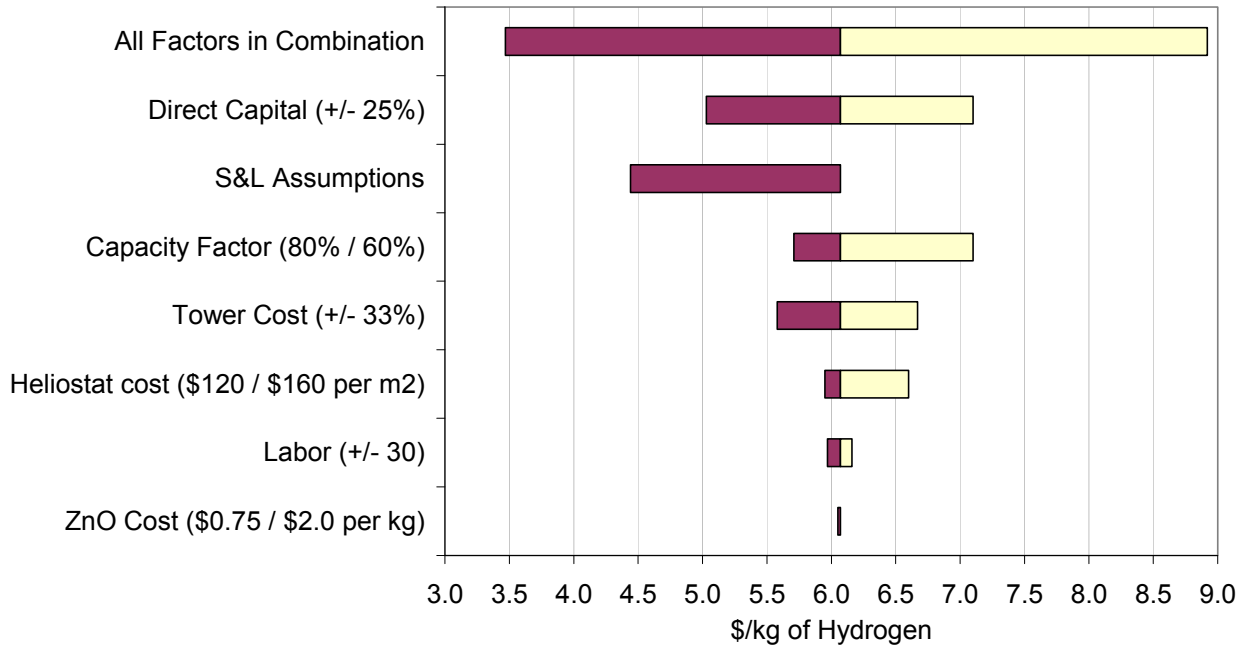

Figure 3-18: ZnO Single variable sensitivity analysis, 2015 Case

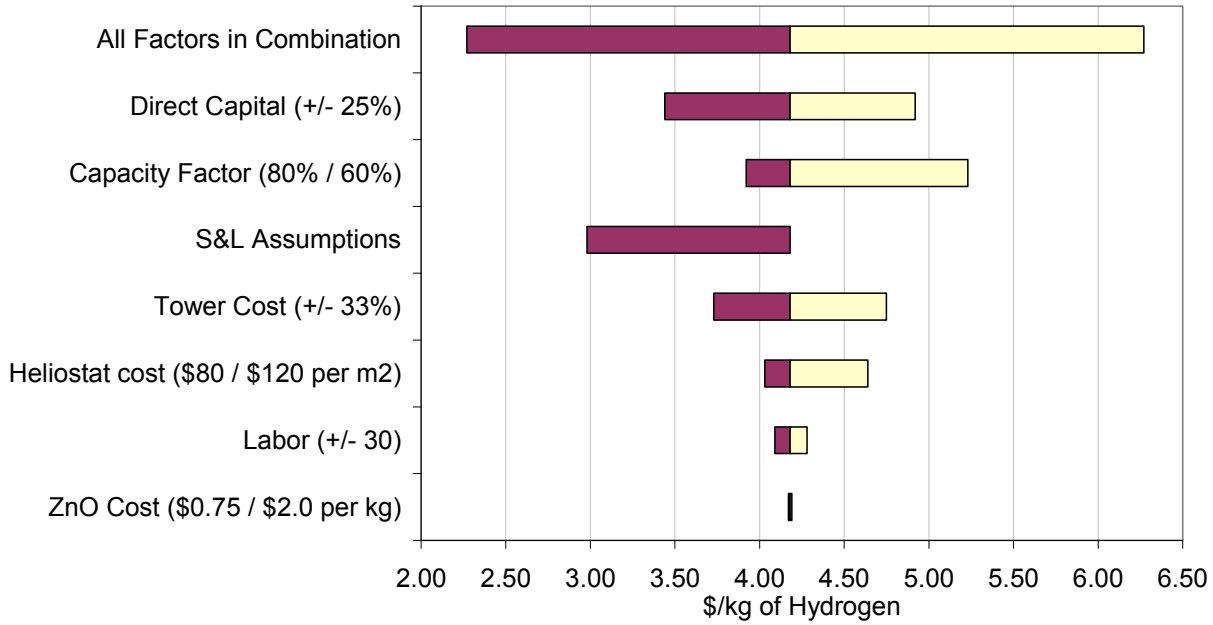

Figure 3-19: ZnO Single variable sensitivity analysis, 2025 Case

3.7 Manganese Oxide (MnO) STCH Process

3.7.1 Overview

Analysis of the manganese oxide (MnO) cycle was conducted by the University of Colorado. The MnO process involves three reactions, summarized in Table 3-27: metal reduction, hydrogen production, and hydrolysis/regeneration.[28] The metal reduction process occurs at temperatures on the order of 1,500 to 1,600 C. Conversion rates of approximately 60 to 80% at residence times of a few seconds have been demonstrated in the laboratory using an aerosol reactor and an inert purge gas to minimize the oxygen concentration in the feed. Hydrogen production occurs at temperatures over 650 C at low pressure, and has been demonstrated with conversion rates of 80 to 90% and residence time of approximately 30 minutes [38].

The cycle is closed by hydrolysis of $NaZnMn_2O_4$ at less than 100 C, followed by the vaporization of NaOH in aqueous solution, and recovery of solid NaOH for use in the hydrogen production step. Experimental results indicate that recovery of NaOH requires a large excess water (10 mol H_2O/mol H_2), which adversely affects the cycle efficiency and kinetics. In addition, side reactions during hydrolysis prevent complete sodium recovery, and 10-20% of sodium has to be carried through the high temperature step, which presents challenges for the reactor design [38]. Recent findings [39] suggest that NaOH may be recovered with a membrane process. If feasible, such a process could make the MnO STCH process considerably more attractive.

Table 3-27: Manganese Oxide Cycle Reaction Summary

Stage	Net Reaction	Notes/Comments
Metal Reduction	$Zn_{0.66}Mn_2O_{3.66} \rightarrow 2Zn_{0.33}MnO_{1.33} + 0.5O_2$	1,500 to 1,600 C, in presence of inert purge gas to minimize O_2
Hydrogen Production	$2Zn_{0.33}MnO_{1.33} + 2NaOH \rightarrow H_2 + Na_2Zn_{0.66}Mn_2O_{4.66}$	>650 C, 0.1 bar, ~30 min residence time
Hydrolysis	$Na_2Zn_{0.66}Mn_2O_{4.66} + H_2O \rightarrow Zn_{0.66}Mn_2O_{3.66} + 2\ NaOH$	Hydrolysis at <100 C, followed by NaOH recovery in excess H_2O. May be possible to recover NaOH using a membrane separator.

3.7.2 Plant Design

Energy to drive the MnO unit processes is provided by solar thermal energy, which is captured by concentrating sunlight onto a central receiver using heliostat fields. A dedicated set of eight towers (24 heliostat fields) supplies the energy for the high temperature reduction reaction, which occurs only on-sun (i.e., during daylight hours). Each tower is coupled to a dedicated reduction reactor module, which includes the reactor itself, heat integration equipment, and an Argon/Oxygen separation unit. The two lower temperature reactions (hydrogen formation and hydrolysis/NaOH separation) occur in a single centralized plant that operates 24 hours per day. Energy for the low temperature reaction is provided by a hot sand thermal storage system, which

[28] As initially conceived, the MnO oxide process used pure MnO. However, it was found that addition of a secondary metal (e.g., zinc or iron) aided in the recovery of NaOH by reducing the amount of excess water. The system that is presented here uses a 3:1 Mn to Zn ratio.

is heated during daylight hours by a solid particle receiver. Solids are transported between the low-temperature plant and the reduction reactions using a pneumatic transport system. An illustrative layout of the MnO (solar + chemical) plant is shown in Figure 3-20, and a summary of key solar plant characteristics is shown in Table 3-28 (for the high temperature thermal reduction plant) and Table 3-29 (for the low- and medium temperature hydrolysis/hydrogen production plant).

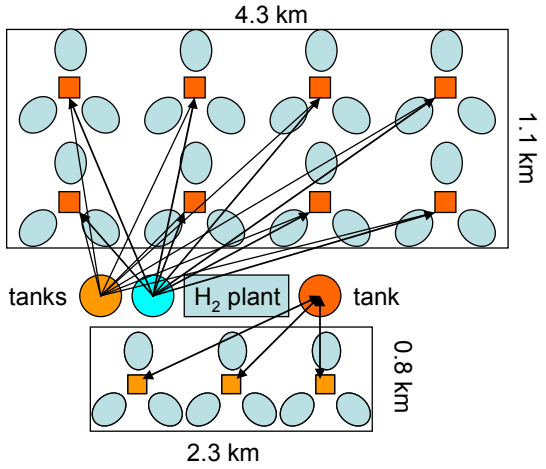

Figure 3-20: Illustrative layout of MnO STCH plant [38]

Table 3-28: Summary of MnO high-temperature solar plant operational characteristics (Reduction Reaction)

Parameter	2015	2025
Design point (TPD H_2)	100	100
Heliostat area	2,485,000 m^2	2,485,000 m^2
Secondary concentrator	3,200 m^2	3,200 m^2
Tower height	221 m	181 m
Number of towers	8	3
Number of solar fields	3 per tower	3 per tower
Solar field efficiency	?	?
Solar auxiliaries	-	-
Thermal Storage	13 hr supply of reactant	13 hr supply of reactant
Max temperature	1,600 C (metal reduction);	1,000C
Receiver (Avg)	~1,200 MWth average	~325 MW_{th} average

Table 3-29: Summary of MnO low and medium-temperature solar plant operational characteristics (Hydrolysis & H_2 Production Reactions)

Parameter	2015	2025
Design point (TPD H_2)	100	100
Heliostat area	1,030,000 m^2	1,030,000 m^2
Secondary concentrator	3,200 m^2	3,200 m^2
Tower height	181 m	181 m
Number of towers	3	3
Number of solar fields	3 per tower	3 per tower
Solar field efficiency	?	?
Solar auxiliaries	-	-
Thermal Storage	Approx 1,400 MW_{th} hot sand, 13 hrs	Approx 1,400 MW_{th} hot sand, 13 hrs
Max temperature	1,000C	1,000C
Receiver (Avg)	~325 MW_{th} average	~325 MW_{th} average

The MnO chemical process was modeled using Aspen Plus. A simplified diagram of the resulting flowsheet is shown in Figure 3-21. The high temperature reduction reaction occurs in aerosol flow reactors that are directly heated by solar thermal energy during daylight hours. Prior to entering the reactor, the metal oxide ($ZnMn_2O_4$) is preheated and finely dispersed in an Argon carrier gas. Following the reaction, the solid ZnMn2O3 product is quenched to 800C to prevent back reaction, separated from the carrier gas/oxygen mixture using a simple metal filter, and stored for subsequent around-the-clock use in the hydrogen production stage. The quench step has not yet been evaluated to determine how rapidly the quench needs to occur, so the amount of heat recoverable from the quench is uncertain (50% is assumed). In order to recycle the carrier gas, the analysis assumes that a ceramic oxygen transport membrane is used to separate argon from oxygen. However, these systems are not commercially available, and the analysis does not account for their cost. The assumed conversion rate for the reduction step is 80%, which is at the high end of the demonstrated laboratory tests.

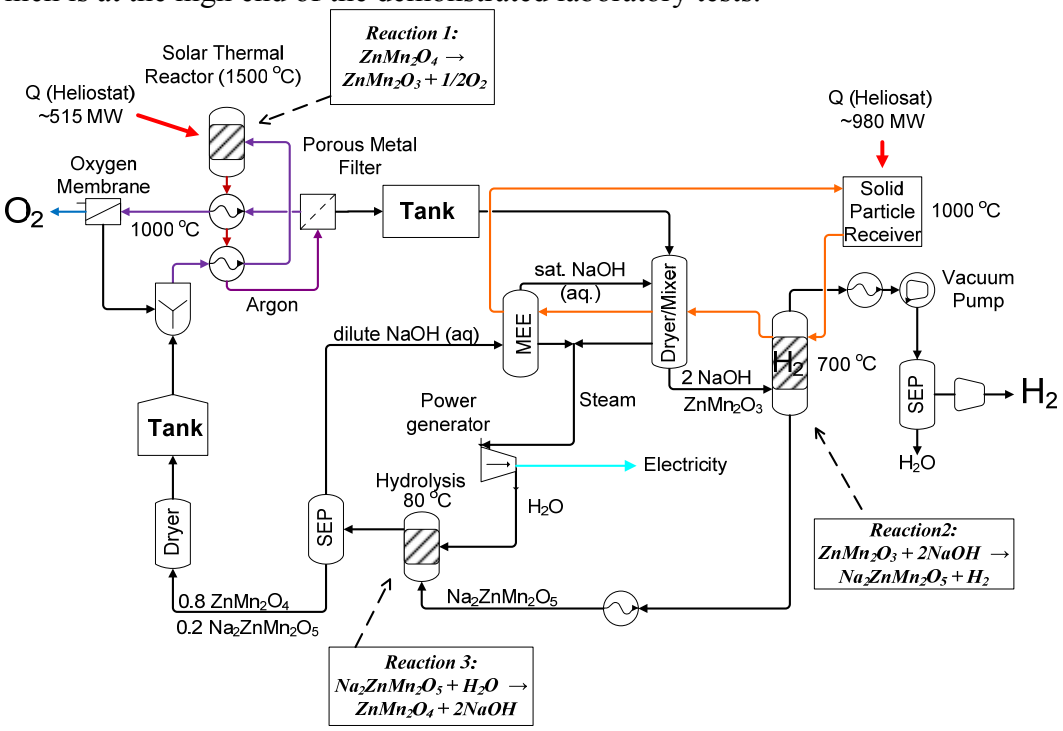

Figure 3-21: MnO process flowsheet [38]

The hydrogen production step entails (1) mixing the reduced oxides (stored at 800 C following the high temperature reaction) with concentrated NaOH; (2) vaporizing the solution in the dryer to form a solid NaOH/oxide mixture; and (3) reheating the solids to 650 C in a low pressure environment (0.1 atm), during which hydrogen is generated. The hydrogen conversion rate is assumed to be close to 100%, which has not been demonstrated with the mixed metal oxide system, and is modeled as a continuous process, which may be problematic given the long residence time and required low pressure environment. The hydrolysis reaction occurs at low temperature in a large excess of water. The subsequent separation of NaOH occurs in a multi-effect evaporator system. Sodium recovery is assumed to be 80%.

A summary of key chemical plant operational characteristics is shown in Table 3-30.

Table 3-30: Summary of MnO chemical plant operational characteristics

Parameter	2015	2025
Design point (TPD)	133	133
Max temperature	1,500 to 1,600 C	1,500 to 1,600 C
# of reactions	3	3
Reduction reactor	8 Aerosol flow reactors	8 Aerosol flow reactors
Hydrolysis reactor	1 low pressure vessel continuous reactor	1 low pressure vessel continuous reactor
Duty cycle (hrs per day)	8 hrs (reduction) 24 hrs (hydrolysis & H_2 production)	8 hrs (reduction) 24 hrs (hydrolysis & H_2 production)
Thermal energy use	92 kWh/kg H_2	92 kWh/kg H_2
Auxiliaries energy use	3 kWh/kg H_2	3 kWh/kg H_2
# of laborers (solar + chem)	135	135
STCH efficiency[29]	34%	34%

3.7.3 Capital & Operating Costs

The capital and operating costs for the MnO process are summarized in Table 3-31. A full analysis of a 2025 case was never developed, although the 2015 cost analysis was re-run for the lower cost 2025 heliostat field and electricity cost. Due to technical challenges, work was halted on the cycle before the final results could be fully reviewed and validated by TIAX. The analysis that was developed appears to be based on reasonable assumptions and is largely consistent with the other analyses. Information on the precise cost basis for many of the chemical plant components was not provided, but the data looks generally reasonable, and is similar in many respects to analysis that was conducted on the ZnO process.

To harmonize the results with more recent analyses, several changes were made to the H2A spreadsheet provided by the University of Colorado. These changes include: (1) updating costs to 2007$; (2) modifying indirect cost calculations to reflect updated assumptions; (3) modifying the cost of thermal storage to \$20/kWh_{th}, which is consistent with more recent data; and (4) revising heliostat costs upward (explained below). Several additional outstanding issues related to the MnO analysis are noted below. It should also be noted that there may be potential for utilizing a membrane separation technique to recover sodium, which would make the economics of the MnO process significantly more attractive.

[29] See section 2.3 for definition of solar-to-heat efficiency

Table 3-31: MnO STCH cycle capital and operating costs

Category	2015	2025	Comments
Solar Plant Installed Capital Costs			
Heliostats	$446	$316	$127/m^2 (2015), $90/m^2 (2025) [6]
Tower	$155	$155	3 181m towers, 8 223m towers; Scaled from [4]
Receiver	$15	$15	Falling sand receiver, used for low temp rxns [16]
CPC	$4	$4	Assumed 10X heliostat cost
Thermal Storage	$28	$28	$20/kWh$_{th}$, 1,400 MW$_{th}$ [17,18,19]
Controls	-	-	
Balance of Plant	-	-	
Total Solar Cost	**$648**	**$518**	**Sum of the above**
Chemical Plant Installed Capital Costs			
Evaporator	$0.9	$0.9	Used for NaOH separation
Compressors	$21	$21	
Storage Tanks	$6.8	$6.8	
Separators	$0.4	$0.4	
Filter	$2.0	$2.0	
Low Temp. Reactors	$1.4	$1.4	Hydrolysis & H_2 Production reactor
Reduction Reactors	$4.4	$4.4	
Conveyors	$4.5	$4.5	
Dryers	$0.6	$0.6	
Heat Exchangers	$33	$33	
Initial Chemicals Cost	$14	$14	Includes NaOH, MnO, ZnO, and Ar
O_2 Transport Membrane	-	-	Not included in cost analysis
Chemical Plant Cost	**$89**	**$89**	Sum of the above
Chemical Plant Installed Capital Costs			
Total Direct Capital	$737	$607	Sum of chemical & solar plant cost
Indirect Capital	$274	$226	Includes contingency, fees, engineering & design, site preparation, and land cost
Total Capital Cost	**$1,011**	**$833**	Sum of indirect & direct capital
Annual Operating Cost			
Fixed op costs	$34	$32	Includes labor, prop taxes, insurance, maintenance & repairs.
Variable op costs	$9	$6	Includes electricity & water
Total Operating Cost	**$43**	**$37**	**Sum of fixed and variable operating costs**

Outstanding issues related to the MnO cost estimation include the following:

- **Oxygen separation membrane**: The cost of the membrane separation module for Ar/O_2 separation was not accounted for because large scale modules are not commercially available and no reasonable comparison was available. A vacuum swing adsorber similar to that used for the ZnO system could be used, which would add to the capital cost and would significantly increase the electricity requirement.
- **Heliostat cost & sizing:** The costs reported for the low/medium temperature heliostat field were significantly smaller than they should have been given the field size of 1,050,000 m^2. (They may have been based on the 2025 cost of $90/m^2). This value was revised upwards.
- **Chemical plant equipment cost basis:** The cost basis for many of the items in the chemical plant is unclear.
- **Solar plant auxiliary electricity use:** Does not appear to be accounted for.

- **Thermal losses and solids transport:** Heat losses during transport and storage of the hot materials are not accounted for.

3.7.4 Results

A summary of the hydrogen cost projected by the manganese oxide H2A analysis is shown in Table 3-32. As shown, the 2015 case is close to the near-term target of $5 to $6 per kg, while the 2025 case is approximately 50% higher than the long-term target of $2 to $3 per kg. As shown in Table 3-31, the bulk of the direct capital expense consists of the solar plant, for which the heliostats and towers are the primary cost driver.

Table 3-32: Zinc Oxide Cycle Hydrogen Cost Breakdown

Analysis Year	Capital	Fixed O&M	Var O&M	Total	Critical Assumptions
2015	$4.41	$0.96	$0.25	**$5.62**	- Reduction step: 80% conversion; 50% of heat recovered from quench - Hydrogen prod step: 100% yield, continuous process - O_2 transport membrane for Argon recycle - 80% Na recovery; reactions unaffected by sodium deposits and/or back reactions - $127/m^2 heliostat cost
2025	$3.64	$0.89	$0.16	**$4.68**	- Chemical process: Same as 2015 - $90/m^2 heliostat cost

3.8 Cadmium Oxide (CdO) STCH Process

3.8.1 Overview

Analysis of the cadmium oxide (CdO) was conducted by General Atomics (GA). The cadmium oxide cycle consists of two reaction steps and a quench step, summarized in Table 3-33. For this embodiment of the process, the cadmium decomposition occurs at high temperature in an air carrier. However, using an inert carrier gas (such as Helium) may potentially allow for lower temperature operation. The decomposition step has been demonstrated in the laboratory, but not in a solar thermochemical reactor. The decomposition is followed by a yet-to-be defined quench step, which is needed to halt the recombination of cadmium and oxygen back to cadmium oxide. The cycle is closed with a cadmium hydrolysis reaction, in which hydrogen is produced from molten cadmium, followed by the separation of hydrogen using a palladium membrane. The hydrolysis step has been demonstrated at atmospheric pressure; however integration of the process at higher pressure with the hydrogen separation step is ongoing [40, 41].

Table 3-33: Cadmium Oxide Cycle Reaction Summary

Stage	Net Reaction	Notes/Comments
Cadmium Decomposition	CdO → Cd(g) + ½O2(g)	1450°C, On-sun only
Cadmium Vapor Quenching	Cd(g) → Cd(l)	1450 → 700°C, halts back reaction
Cadmium Hydrolysis	Cd(l) + H2O → CdO + H2	460°C, 24 hrs per day

3.8.2 Plant Design

A block diagram of the cadmium oxide process is shown in Figure 3-22. Due to the high temperature requirement, the decomposition step occurs only on-sun. The quenched molten cadmium product is stored at 700 C for eventual use in the hydrolysis reaction. Heat from the molten cadmium at 700 C is used to drive a turbine to power the plant auxiliaries and cool the product to the desired hydrolysis temperature of 460 C. The CdO product from the hydrolysis reaction is stored overnight for use in the decomposition reactor during daylight hours.

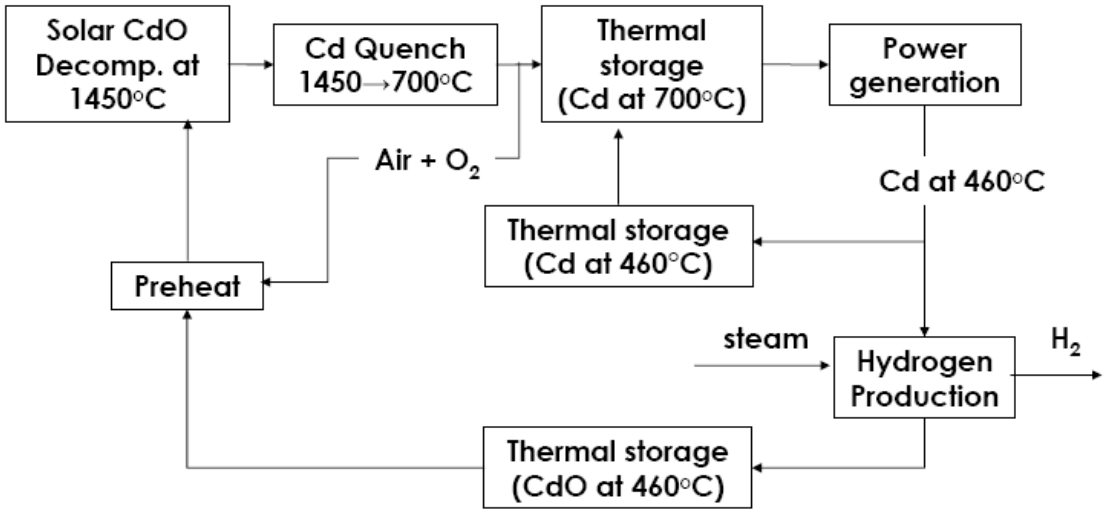

Figure 3-22: Cd/CdO process block diagram [40]

The CdO plant is designed to integrate with a solar field using a beam-down field configuration. In a beam-down configuration, solar power is concentrated from a heliostat field to a single downward-facing reflector on a power tower, where it is then reflected to a secondary concentrator and thermal receiver located on the ground. The beam-down configuration simplifies some aspects of handling cadmium, which is toxic, but adds additional complexity and reduces the efficiency of the solar field. The solar plant was designed based on research and demonstration conducted at the Weizmann Institute [42]. The heliostats are configured in a surround-field configuration, as shown in Figure 3-23. There remain several unanswered questions related to the specified field design, which are noted in our discussion of plant capital costs. A summary of the solar field characteristics is shown in Table 3-34.

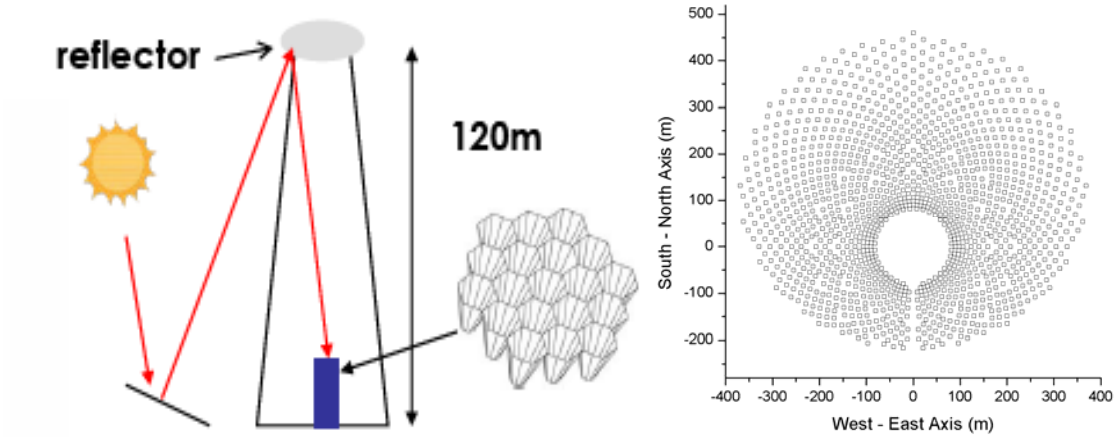

Figure 3-23: Beam-down field configuration (Left) and CdO heliostat field layout (right) [41]

Table 3-34: Summary of Sulfur-Ammonia solar plant operational characteristics

Parameter	2015	2025[30]
Design point (TPD H_2)	133[31]	N/A
Heliostat area (m^2)	1,702,000	N/A
Secondary concentrators (m^2)	41,850	N/A
Tower Reflector (m^2)	50,850	N/A
Tower height (m)	124 m	N/A
Number of towers	10	N/A
Number of solar fields	1 per tower	N/A
Solar field efficiency	62%[32]	N/A
Solar auxiliaries (MW_e)	5 MW_e	N/A
Thermal Storage	Molten Cd	N/A
Max temperature	1,450 C	N/A
Receiver (MW_{Th}, peak)	73 MW_{th} per receiver	N/A

The decomposition reaction and quench are designed to occur in a reactor similar to that shown in Figure 3-24 (left figure): the decomposition reaction occurs in a thermal receiver over a fluidized CdO bed, which helps improve the reaction kinetics. The quench happens at the outlet of the reactor and is assumed to use molten cadmium. As discussed above, the optimum quench

[30] No analysis was conducted for a 2025 case
[31] It appears that the solar plant was designed for 133 TPD of hydrogen production
[32] The solar field calculations may not have included thermal losses in the receiver, which could further reduce efficiency on the order of 20%

approach has not yet been determined. The hydrolysis reactor concept (Figure 3-24, right) uses a rotating reactor at pressures on the order of 50 bar, with molten cadmium and steam flowing in opposite directions. The high pressure is necessary to reduce the reactor size, but high pressure operation has not yet been demonstrated for either the hydrolysis reaction or the hydrogen separation stage. As shown, after hydrogen is recovered from steam, the steam is recycled to the reactor steam inlet. Each of the ten solar power towers is coupled to a decomposition reactor; reactants are transported to two chemical plants that include the hydrolysis reactor. Solid CdO from the hydrolysis reactors is conveyed via bucket conveyors to thermal storage hoppers, where it is stored. It is dispensed to the decomposition reactor via pneumatic conveyors during solar plant operation [40, 41].

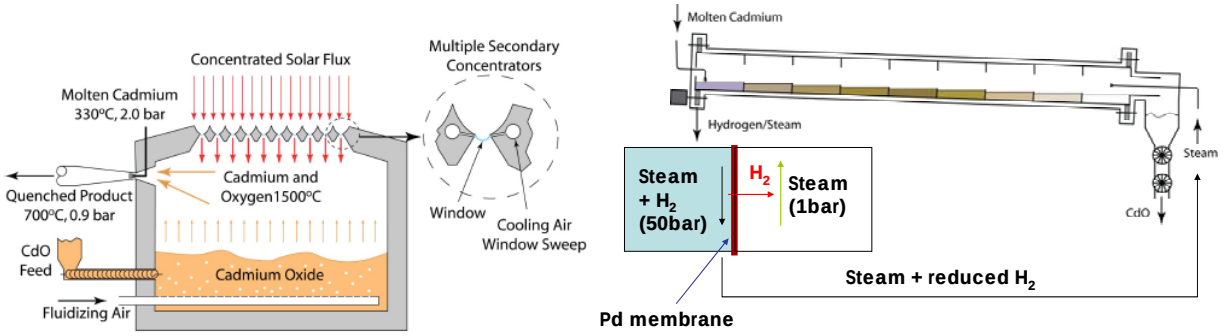

Figure 3-24: Conceptual diagram of CdO decomposition reactor (left) and hydrolysis reactor (right) [40]

Table 3-35: Summary of CdO chemical plant operational characteristics

Parameter	2015	2025[33]
Design point (TPD)	133	N/A
Max temperature	1,450	N/A
# of reactions	2	N/A
Cd decomposition reactor	10 fluidized bed reactors	N/A
Hydrolysis reactor	2 rotating counter flow reactors, 50 bar	N/A
Duty cycle (hrs per day)	8 hrs (CdO decomposition) 24 hrs (hydrolysis)	N/A
Thermal energy use	55.9 kWh/kg H_2	N/A
Auxiliaries energy use	0.1 kWh/kg H_2	N/A
# of laborers (solar + chem)	78	N/A
STCH efficiency[34]	59%	N/A

3.8.3 Capital and Operating Costs

Due to funding constraints, the cadmium oxide economic analysis was never fully completed. As such, we are unable to provide a fair comparison of the CdO to the other analyses. However, we have included a summary of the major capital and operating costs Table 3-36. The data is presented "as is": i.e., it represents the most recent cost information supplied to TIAX by General Atomics, adjusted to 2007$, but it has not been fully vetted by TIAX or DOE. Below the table, we have included comments that identify the major outstanding questions related to the CdO economic analysis. It should be stressed that many of the issues identified may have been

[33] No analysis was conducted for a 2025 case
[34] See section 2.3 for definition of heat-to-hydrogen efficiency

addressed in the analysis conducted by General Atomics – however, we have not been provided with the information to adequately comment.

Table 3-36: CdO STCH cycle capital and operating costs

Category	2015	2025[35]	Comments
Solar Plant Installed Capital Costs			
Heliostats	$241	N/A	$127/m^2, 1.7 km^2 [6]
Reflectors	$66	N/A	Weizmann Institute [42]
Secondary Concentrators	$37	N/A	Weizmann Institute [42]
Towers	$66	N/A	Weizmann Institute [42]
Thermal Storage	$28	N/A	Molten Cd storage – Preliminary estimate
Controls	-	N/A	None included
Balance of Plant	-	N/A	None included
Total Solar Cost	**$424**	N/A	**Sum of the above**
Chemical Plant Installed Capital Costs			
CdO Reactor	$9	N/A	10 fluidized bed reactors
Hydrolysis Reactor	$5	N/A	2 rotating counter-current reactors (nickel)
H_2 Separation Membrane	$5	N/A	Palladium membrane, cost estimate from Osmionics
Separators	$5	N/A	5 flash reactors
CdO Thermal Storage Hopper	$9	N/A	Storage for solid CdO from the hydrolysis reactor
Solids conveying	$8	N/A	Bucket conveyors & pneumatic conveyors from
Pumps & Compressors	$16	N/A	
Heat Exchanger	$36	N/A	8 heat exchangers - Heat integration between decomposition reactors, hydrolysis reactors, and thermal storage media
Turbines	$15	N/A	5.8 MW turbine to power plant auxiliaries
Cadmium	$28	N/A	$1.7/kg Cd, 3 day supply
Hydrogen Compression	$17	N/A	6 stage compressor to go to 20 bar
Chemical Plant Cost	**$125**	N/A	Sum of the above
Chemical Plant Installed Capital Costs			
Total Direct Capital	$576	N/A	Sum of chemical & solar plant cost
Indirect Capital	$206	N/A	Includes contingency, fees, engineering & design, site preparation, and land cost
Total Capital Cost	**$782**	N/A	Sum of indirect & direct capital
Annual Operating Cost			
Fixed op costs	$32	N/A	Includes labor, prop taxes, insurance, maintenance & repairs.
Variable op costs	$3	N/A	Includes electricity & water
Total Operating Cost	**$35**	N/A	**Sum of fixed and variable operating costs**

Solar field sizing and efficiency: The solar field is sized to produce 133 TPD of hydrogen (not 100 TPD of hydrogen), so it is oversized. However, the solar efficiency calculations do not appear to account for any losses associated with the receiver/decomposition reactor, which might typically be on the order of 80%, or field availability down time (typically ~1%). In combination, these two factors likely mitigate each other, in which case the solar field size would be close to the appropriate level.

[35] No analysis was conducted for a 2025 case

Beam down design cost estimates: With the exception of the heliostats, the cost estimates for the solar plant beam-down design are based on proprietary cost analysis conducted by the Weizmann Institute. Neither TIAX nor DOE had the opportunity to review this information, so we are unable to verify that the data presented offers a fair basis for comparison to the other cost analyses presented. Some of the questions that were raised during the course of the review are: (1) whether the design includes contingency for operational constraints such as stormy or high wind conditions (e.g., raising and lowering the reflector); (2) the validity of and approach for extrapolating the tower costs to higher tower heights (originally conducted for 68 m, not 110 m towers); (3) cooling of ground-based compound parabolic concentrators (CPCs) (the design indicates that water-cooled concentrators are used, but it is not clear how this implemented); (4) whether the solar costs include balance of plant assumptions, installation factors, etc that are consistent with other analyses.

Reactor cost estimates: Both the hydrolysis reactor and decomposition reactor cost estimates may be understated. The hydrolysis reactor is rated to 50 atm and manufactured from nickel alloy. As a point of reference, a simple horizontal vessel with the appropriate dimensions and these characteristics is estimated by CAPCOST at $11M per reactor (i.e., $22M total). The hydrolysis reactor concept is more complex than a simple vessel, so we would consider that $22M brackets the low-end cost – significantly higher than the $5M estimate that is included.

We were not furnished with information detailing the design characteristics of the decomposition reactor such as the size or materials of construction. However, we speculate that the total decomposition reactor cost of $9M is understated. The plant design includes ten reactors (one per tower) which need to be resilient to high temperatures (1,450 C), corrosive materials (molten Cd), and daily thermal cycling.

Materials handling: Cadmium is toxic, which presents challenges to plant operations. The plant includes enclosed conveyors to transport solid cadmium oxide throughout the plant. However, it is not clear that the current design includes adequate measures to fully address safety questions. These include whether any additional safety systems, decommissioning costs, or fees are associated with operating a plant that uses so much of a toxic substance.

Thermal Storage: The storage costs for molten cadmium were never adequately justified, and we are unsure if thermal losses were accounted for.

Separation membrane: The cost analysis appears to include a single separation membrane, but the plant design includes two hydrolysis reactors. It is not clear if membrane durability has been addressed in the cost analysis.

3.9 Sulfur-Iodine (S-I) STCH Process

3.9.1 Overview

Analysis of the sulfur-iodine (S-I) water splitting process was conducted by General Atomics, and leverages previous work conducted for the nuclear hydrogen initiative [43, 44]. The sulfur-iodine cycle for hydrogen production is depicted in Table 3-37. The process consists of three chemical reactions. The first reaction entails sulfuric acid decomposition, producing sulfur dioxide and oxygen. This is followed by the Bunsen reaction, in which sulfuric acid and hydriodic acid are formed. In the third reaction, hydriodic acid is separated from the other components and decomposed into hydrogen and iodine [45].

Table 3-37: Sulfur Iodine Cycle Reaction Summary

Stage	Net Reaction	Notes/Comments
Sulfuric acid decomposition	$H_2SO_4 \rightarrow 0.5O_2 + SO_2 + H_2O$	800 to 900C, 6 bar. Occurs in bayonet heat exchanger/reactor
Bunsen reaction	$2H_2O + SO_2 + I_2 \rightarrow H_2SO_4 + 2HI$	Spontaneous at <120 C
Hydriodic acid decomposition	$2HI \rightarrow I_2 + H_2$	Separation & decomposition of HI 300 C

The process was fully demonstrated piece-wise at General Atomics in the 1970s and '80s, including the demonstration of a concentrated solar decomposer in which sulfuric acid was decomposed on top of a solar power tower. The complete cycle has subsequently been demonstrated in continuous operation under projected operating conditions. Some of the key challenges associated with the S-I process include the handling of corrosive chemicals (H_2SO_4, HI); the use of iodine; the large reactant recycle streams; and the difficulty associated with HI decomposition [45].

3.9.2 Plant Design

The sulfur-iodine cycle was developed primarily through the nuclear hydrogen initiative (NHI) and was subsequently adapted for solar thermal operation. To adapt the process for solar operation, GA designed the process to utilize solar thermal energy to drive the decomposition reaction and electricity to provide the thermal energy requirement for HI decomposition and to power plant auxiliaries. Due to its similarities with the hybrid-sulfur process,[36] GA's S-I analysis utilizes a scaled version of the solar plant used for the 2015 Hy-S analysis.[37] Additional plans were in place to develop a customized solar plant similar to the beam-down design using the CdO cycle, but this modified design was never reviewed by TIAX or presented to DOE.

The sulfur-iodine chemical process flowsheet was generated by General Atomics using Aspen Plus. Sulfuric acid is decomposed into SO_2, O_2 and water in bayonet heater reactors similar to that described for hybrid-sulfur process. The heat requirement for the high temperature decomposition reaction is provided by hot sand thermal storage using circulated air at 1 bar as a

[36] The sulfur decomposition step – which has the highest temperature requirement and uses the bulk of the process energy –is identical for both the S-I and HyS processes.

[37] Solar thermal energy is collected using a particle receiver mounted on a solar power tower and stored in a hot sand storage medium to enable 24-hour plant operation. The solar field was designed using DELSOL.

heat transfer medium.[38] The decomposition products are sent to a Bunsen reactor module, along with HI, iodine and water from the hydriodic acid decomposer modules, where they are reformed into sulfuric acid and hydriodic acid. No additional heat is required to drive the Bunsen reactor modules. The thermal energy requirement for the hydriodic decomposition module is provided by electricity, which drives heat pumps to boost the operating temperature. Extensive heat is recovered from the HI decomposition products. Utilizing electricity for this stage of the reaction decouples the HI decomposition operation from the sulfuric acid decomposition, which simplifies plant integration [45, 46].

A separate chemical plant (i.e., a sulfuric acid decomposer module, a Bunsen reactor module, and a hydriodic acid decomposer module) is coupled to each of the two power towers. A summary of key chemical plant operational characteristics is shown in Table 3-38.

Table 3-38: Summary of S-I chemical plant operational characteristics

Parameter	2015	2025[39]
Design point (TPD)	133	N/A
Max temperature	900	N/A
# of reactions	3	N/A
# of chemical plants	2 (One per tower)	N/A
Duty cycle (hrs per day)	24 hrs	N/A
Thermal energy use	?	N/A
Electricity	?	N/A
# of laborers (solar + chem)	?	N/A
STCH efficiency[40]	35% (unverified)	N/A

3.9.3 Results

While GA completed a process flowsheet and an H2A analysis for the S-I STCH case, TIAX did not have opportunity to review this analysis, so we are unable to comment. Based on information provided in a white paper issued by General Atomics, the cost of hydrogen in 2005$ was projected to be $4.78/kg for a 2015 case. We did receive information on a similar case study conducted for larger scale (1,000 TPD) nuclear S-I plant, and the analysis for the nuclear case appears to be consistent with the methodology used elsewhere in this report. Using simple scaling laws to appropriately adjust the capital cost of the nuclear case gives a similar hydrogen cost projection to that indicated above (i.e., approximately $5.00 per kg hydrogen for a 2015 case, in 2007$). Using the lower heliostat cost for the 2025 case and leaving other factors as is gives a cost projection of $4.68/kg. However, the nuclear S-I plant does not use electricity to provide the thermal input to the HI reaction, so it is difficult to apply these results to the STCH analysis described above. We have included these cost estimates in the conclusion, but with the caveat that they have not been fully vetted.

[38] High-pressure helium offers an avenue to increase the process efficiency
[39] No analysis was conducted for a 2025 case
[40] See section 2.3 for definition of solar-to-heat efficiency

4 Conclusions

4.1 Summary of STCH Process Results and Critical Paths

Using a common methodology, the economics of producing hydrogen was evaluated for eight different high-temperature solar thermochemical water splitting processes. A summary of key metrics for each of the STCH cycles evaluated is shown in Table 4-1 (2015 case) and Table 4-2 (2025 case). Based on our review, we have summarized the current status and identified critical development pathways towards achieving long-term DOE targets for each individual process:

Hybrid Sulfur: The hybrid-sulfur cycle offers relatively low capital and operating costs, and leverages several known technologies. Successful development requires demonstration of a viable sulfur decomposition reactor (capable of heat recovery and fast kinetics) and a viable electrolysis system. Achieving the DOE long-term cost target would therefore require: (1) A viable electrolysis reactor (high efficiency, low cost, and durable); (2) Low cost renewable electricity; (3) Successful implementation of the 2025 plant concept that uses a low-cost particle receiver and allows direct heat exchange with the decomposition reactor; and (4) Additional cost reductions such as reduced decomposition reactor costs or alternate economic parameters.

Copper Chloride: The copper chloride cycle is attractive in that it can be readily coupled to known solar and chemical plant technologies that have been demonstrated in other applications, suggesting that if the chemistry is successfully demonstrated, there is relatively low technical risk in scaling the process to high volume hydrogen production. The key challenges relate to the relatively low process efficiency; demonstration of a viable (i.e., durable, low cost, high efficiency) electrolysis system, and demonstrating a closed cycle. Achieving the long-term cost targets would likely require: (1) Boosting system efficiency towards 40%; (2) Low cost renewable electricity (<$0.05/kWh); and (3) A viable electrolysis unit that meets the 2025 targets.

Ferrite: The thin film nickel ferrite cycle is attractive due to its relative simplicity (only two reactions), its potential for high process efficiency, and, relative to other metal oxide cycles, its low operating temperature. Critical operational characteristics related to reaction kinetics and materials durability under real-world conditions are still under investigation. The enabling factors towards achieving the DOE long-term cost targets are: (1) Development of highly reactive (~1 minute average residence times) ferrite thin films capable of repeated cycling; (2) Successful development and demonstration of an integrated reactor/receiver that can operate at high temperature and effectively recuperate heat from the process; and (3) Commercial availability of thin film ferrite at a cost in the range of $200 to $400 per kg.

Sulfur-Ammonia: The sulfur-ammonia cycle is still under development. The critical challenges relate to improving process efficiency and development of low cost thermal receivers, as well as demonstrating the closed reaction and developing a viable electrolysis system. Future development of an optimized process flowsheet will provide greater insight into the economics of this system. Like the CuCl process, the S-A system relies primarily on proven chemical and solar plant equipment, which decreases the overall technical risk.

Zinc Oxide: The zinc oxide cycle faces critical challenges related to (1) the propensity of reacted ZnO to dissociate into zinc and oxygen, which adversely affect the process efficiency and economics; and (2) the high reaction temperatures (in excess of 1,700 C). Hence, achieving the long-term cost target would likely require: (1) the 85% net ZnO reaction yield assumed for the 2025 case (well above demonstrated performance); (2) an advanced high temperature reactor that minimizes the carrier gas required; and (3) additional cost reductions – most likely to the power towers, which contribute a significant fraction towards plant capital costs.

Manganese Oxide: The manganese oxide cycle faces significant challenges with respect to sodium recovery, which affects reaction kinetics, cycle efficiency, and can potentially affect reactor operation. Other challenges include effective heat recovery from the high temperature reaction; achieving target process yields; and recovery of the carrier gas following reduction. Critical paths that would enable meeting DOE cost targets include: (1) Development of transport membranes for both sodium separation and Argon/oxygen separation; (2) Demonstration of the assumed reaction yields; (3) Development of a mechanism for minimizing back reactions following the reduction reaction while recovering most of the process heat. Recent developments not captured in the MnO cost analysis suggest that sodium separation via a membrane process may be feasible, which could dramatically alter the viability of this system.

Cadmium Oxide: The Cadmium Oxide economic analysis was never fully completed and validated. However, there are promising aspects (e.g., high efficiency, simple two step process). Some of the critical factors that remain to be investigated are the viability of the proposed beam down solar field design under real-world conditions, the demonstration of the high-temperature fluidized bed reactor and quench process.

Sulfur-Iodine: TIAX was not provided sufficient information to complete analysis.

It should also be stressed that, while the analyses presented in this report use a common basis for economic and system design considerations, the individual cycles differ in terms of: (1) the technical maturity and feasibility of the process itself; (2) the degree to which the results have been optimized to maximize the economic performance; and (3) the extent to which the results assume future improvements in process performance. A detailed evaluation of the feasibility of the processes is beyond the scope of this report. However, in an effort to highlight some of these differences, Table 4-3 summarizes the critical assumptions that form the basis for the 2015 and 2025 analyses, as well as the current status towards achieving these technological milestones.

Table 4-1: Summary of 2015 STCH Cycle Economic Analyses

Parameter	Hy-S	CuCl	Ferrite	S-A	ZnO	CdO	MnO	S-I*
Solar and Chemical Plant Summary								
Heliostat Area (m^2)	1,717,000	1,779,000	2,090,000	3,911,000	2,517,000	1,702,000	3,511,000	?
Thermal Energy ($kWh_{th}/kg\ H_2$)	60.3	65.3	63.9	137.6	82.9	55.9	92	?
Electricity ($kWh_e/kg\ H_2$)	18.5	20.1	-	-	4.7	0.5	3	?
Solar Efficiency	46%	49%	40%	46%	45%	62%	?	?
STCH Efficiency	32%	29%	52%	24%	35%	59%	34%	?
Capital and Operating Cost (M$)								
Solar Plant Capital	$375	$421	$328	$889	$655	$424	$648	?
Chemical Plant Capital	$169	$192	$242	$213	$152	$125	$89	?
Indirect Capital	$187	$208	$183	$399	$290	$206	$274	?
Total Capital Cost[41]	$730	$821	$753	$1,500	$1,097	$782	$1,011	?
Operating Cost (per yr)	$81	$95	$28	$37	$47	$35	$43	?
Hydrogen Cost ($/kg)								
Capital	$3.43	$4.00	$3.27	$6.71	$4.83	N/A	$4.41	N/A
Fixed Operating	$0.70	$1.09	$0.79	$1.03	$0.96	N/A	$0.96	N/A
Variable Operating	$1.54	$1.74	$0.00	$0.00	$0.28	N/A	$0.25	N/A
Hydrogen Price	**$5.68**	**$6.83**	**$4.06**	**$7.74**	**$6.07**	**N/A**	**$5.62**	**$5.01***

*Preliminary estimate based on scaled nuclear case

[41] Includes direct solar, direct chemical, and indirect costs

Table 4-2: Summary of 2025 STCH Cycle Economic Analyses

Parameter	Hy-S	CuCl	Ferrite	S-A	ZnO	CdO	MnO*	S-I**
Solar and Chemical Plant Summary								
Heliostat Area (m^2)	1,370,000	1,779,000	2,090,000	3,325,000	2,394,000	N/A	3,511,000	N/A
Thermal Energy (kWh/kg H_2)	46.9	65.3	63.9	116.9	79.6	N/A	92	N/A
Electricity (kWh/kg H_2)	15.5	18.2	-	-	-	N/A	3	N/A
Solar Efficiency	46%	49%	40%	46%	46%	N/A	?	N/A
STCH Efficiency	39%	30%	52%	28%	42%	N/A	34%	N/A
Capital and Operating Cost (M$)								
Solar Plant Capital	$259	$353	$252	$490	$65	N/A	$510	N/A
Chemical Plant Capital	$135	$163	$88	$164	$512	N/A	$89	N/A
Indirect Capital	$138	$178	$122	$236	$218	N/A	$222	N/A
Total Capital Cost[42]	$532	$694	$461	$890	$794	N/A	$822	N/A
Operating Cost (per yr)	$53	$71	$15	$27	$25	N/A	$37	N/A
Hydrogen Cost ($/kg)								
Capital	$2.38	$3.30	$2.01	$3.89	$3.50	N/A	$3.59	N/A
Fixed Operating	$0.54	$0.98	$0.41	$0.76	$0.67	N/A	$0.88	N/A
Variable Operating	$0.92	$1.11	$0.00	$0.00	$0.01	N/A	$0.16	N/A
Hydrogen Price	**$3.85**	**$5.39**	**$2.42**	**$4.65**	**$4.18**	**N/A**	**$4.63***	**$4.68****

*2025 MnO results reflect only lower heliostat costs compared to the 2015 case

**Preliminary estimate based on scaled nuclear case with lower heliostat cost

[42] Includes direct solar, direct chemical, and indirect costs

Table 4-3: Demonstrated vs Assumed Performance

Process	Current Status - Demonstrated	Critical Assumptions – 2015 Case	Critical Assumptions – 2025 Case
Solar Plant[43]	- $127 to $180/$m^2$ heliostat cost	- $127/$m^2$ heliostat cost	- $90/$m^2$ heliostat cost
Ferrite	- ~15 minute cycle time - ~ 50 cycles demonstrated - Ferrite not commercially available; precursors approximately $225/kg - Reactor concept undemonstrated, materials and operational challenges	- 5 minute average cycle time - 15 year ferrite/substrate lifetime - Ferrite cost = $270/kg - Silicon carbide reactor design w/79% heat recovery	- 1 minute average cycle time - 15 year ferrite and substrate lifetime - Ferrite cost = $270/kg - Silicon carbide reactor design w/79% heat recovery
CuCl	- Electrolyzer uninstalled cost ~$2,500/$m^2$ - 0.7 V, 100 mA/cm^2, ~100 hrs demonstrated - Separations unproven - Materials of construction under evaluation	- Electrolyzer module = 1,140/m^2, uninstalled - 0.7 V, 500 mA/cm^2 electrolyzer, 5 yr lifetime - Closed rxn - Corrosive environment addressed with porcelain-lined equipment	- Electrolyzer module = $950/$m^2$, uninstalled - 0.63 V, 500 mA/cm^2 electrolyzer, 10 yr lifetime - Closed rxn - Corrosive environment addressed with porcelain-lined equipment
ZnO	- 18% overall Zn/ZnO yields (60% for forward rxn only) - High temperature reactor unproven	- 70% Zn/ZnO Conversion (assumes minimal back reactions) - Graphite multi-tube reactor w/high durability	- 85% Zn/ZnO Conversion (no back reactions and improved yields) - Advanced graphite reactor design w/reduced carrier gas & high durability
HyS	- Electrolyzer uninstalled cost ~$2,500/$m^2$ - 0.76 V and 1,100 mA/cm^2, ~50 hrs demonstrated - Catalyst development ongoing - Intermediate heat transfer loop - Small-scale demonstration of falling sand receiver	- Electrolyzer module = $1,140/$m^2$, uninstalled - 0.6 V, 500 mA/cm^2 electrolyzer, 5 yr lifetime - Catalyst development - Intermediate heat transfer loop - Viable falling sand particle receiver	- Electrolyzer module = $300/$kW_e$ (uninstalled) - 0.5 V, 500 mA/cm^2 electrolyzer, 10 yr lifetime - Catalyst development - Elimination of intermediate heat transfer - Viable falling sand particle receiver
S-A	- Electrolyzer uninstalled cost ~$2,500/$m^2$ - 0.7 V, 100 mA/cm^2 - Closed Rxn undemonstrated…	- Electrolyzer module = 1,140/m^2, uninstalled - 0.7 V, 100 mA/cm^2, 5 yr electrolyzer lifetime - Closed rxn	- Electrolyzer module = $950/$m^2$, uninstalled - 0.4 V, 500 mA/cm^2, 10 yr electrolyzer lifetime - Closed rxn
MnO	- Reduction: 60 to 80% conversion; quench not demonstrated - Hydrogen Prod: 80 to 90% yield, batch process - O2 transport membrane not commercially available - Effect of unrecovered sodium on reaction kinetics and durability is unknown	- Reduction step: 80% conversion; 50% of heat recovered from quench - Hydrogen prod step: 100% yield, continuous process - O_2 transport membrane for Argon recycle - Reactions unaffected by sodium deposits and/or back reactions	Same as 2015 Case
CdO	- High temperature reactor not demonstrated - Quench process undefined - Beam down field design un-validated for operational conditions - Permitting & materials handling challenges - Hydrolysis at atmospheric pressure	- Fluidized bed reduction reactor demonstrated - Rapid CdO quench feasible - Cost-effective and robust beam down solar field design - Cadmium toxicity issues addressed - Hydrolysis/hydrogen separation at high pressure (50 bar)	N/A
S-I	- Has been demonstrated as a nuclear thermal process	- Sulfur decomposition catalyst kinetics - Durability & materials handling	N/A

[43] Applies to all analyses

4.2 Cross-Cutting Conclusions

A breakdown of the major cost contributors[44] (the solar plant capital cost, the chemical plant capital cost, the variable operating cost, and the fixed operating cost) for each of the cases analyzed is shown in Figure 4-1 and Figure 4-2. The results of this breakdown may be summarized as follows:

- **Solar & Chemical Plant Capital Costs:** The single biggest contributor to the cost of hydrogen is the initial cost of the solar field used to generate thermal energy, and in particular, the initial capital cost of heliostats. Depending on whether the process in question uses electricity to drive any unit processes (e.g., electrolysis, or as a thermal energy source), the solar plant tends to account for 70 to 90% of the initial capital cost, and 30 to 60% of the total cost of hydrogen, while the chemical plant tends to account for 10 to 20% of the total cost of hydrogen. For processes that use a large amount of electricity and for the 2025 cases (which include significant reductions in the cost of heliostats), the solar plant cost contribution tends to lie at the lower end of this spectrum.
- **Variable Operating Cost:** Variable operating costs are comprised primarily of purchased electricity. In general, the electricity needed to power plant auxiliaries is relatively minor. Hence, the importance of the variable cost contribution is driven by (1) Whether the process in question uses electricity to drive any of the unit processes; and (2) The assumed cost of electricity ($83/MWh in 2015, and $58/MWh in 2025).
- **Fixed Operating Cost:** Fixed operating costs are comprised primarily of O&M costs (which are primarily a function of the initial capital cost of the chemical plant) and labor costs. There is relatively little variation in this cost component between the different analyses.

Given the importance of the cost of the solar plant to the total selling price, process enhancements that increase the cycle's thermal efficiency (and hence reduce the overall size of the heliostat field), and technology improvement opportunities that reduce the initial cost of heliostats are critical enablers for the eventual commercial success of STCH production.

[44] Indirect costs are assigned proportionately to the solar and chemical plant portions of each cost analysis.

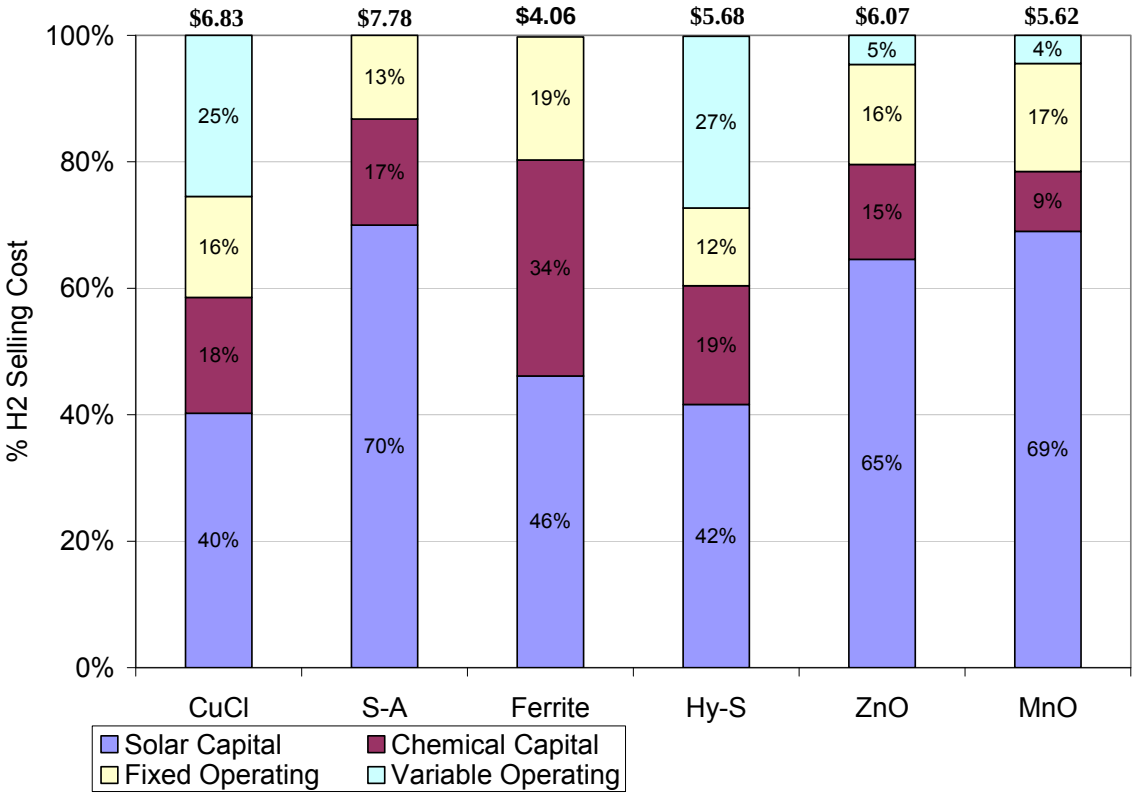

Figure 4-1: 2015 Summary Cost Breakdown

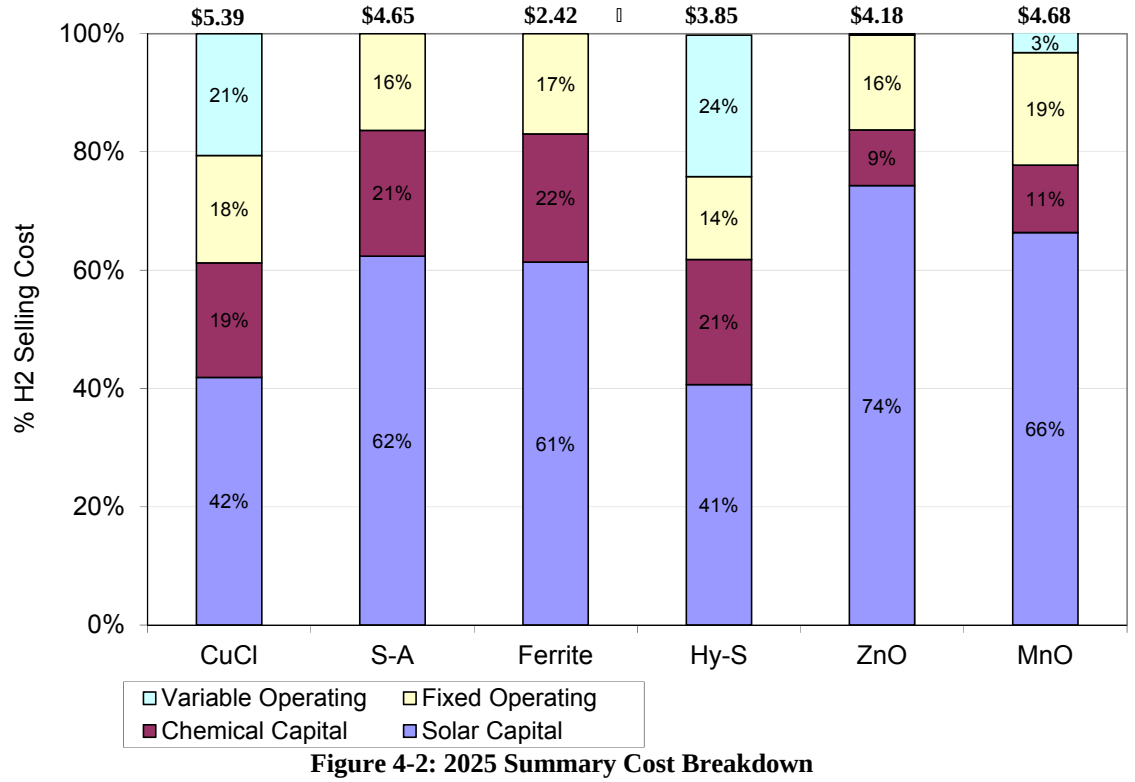

Figure 4-2: 2025 Summary Cost Breakdown

Finally, based on the results of this analysis, we can provide several cross-cutting comments with respect to the overall project:

1. Heliostats costs are the primary cost driver for all of the processes that were analyzed. As such, measures that increase plant efficiency (i.e., reduce the plant thermal requirement and hence the size of the solar field) or decrease the heliostat unit cost offer a high return on investment. Heliostat costs that meet or exceed the 2025 target of $90/m^2 appear to be a prerequisite for any of the STCH cycles to meet the long-term DOE goals. This relationship between cycle efficiency, heliostat cost, and the projected hydrogen selling price is illustrated in Figure 4-3 (the primary difference between the 2015 and 2025 cases is the cost of the heliostat).

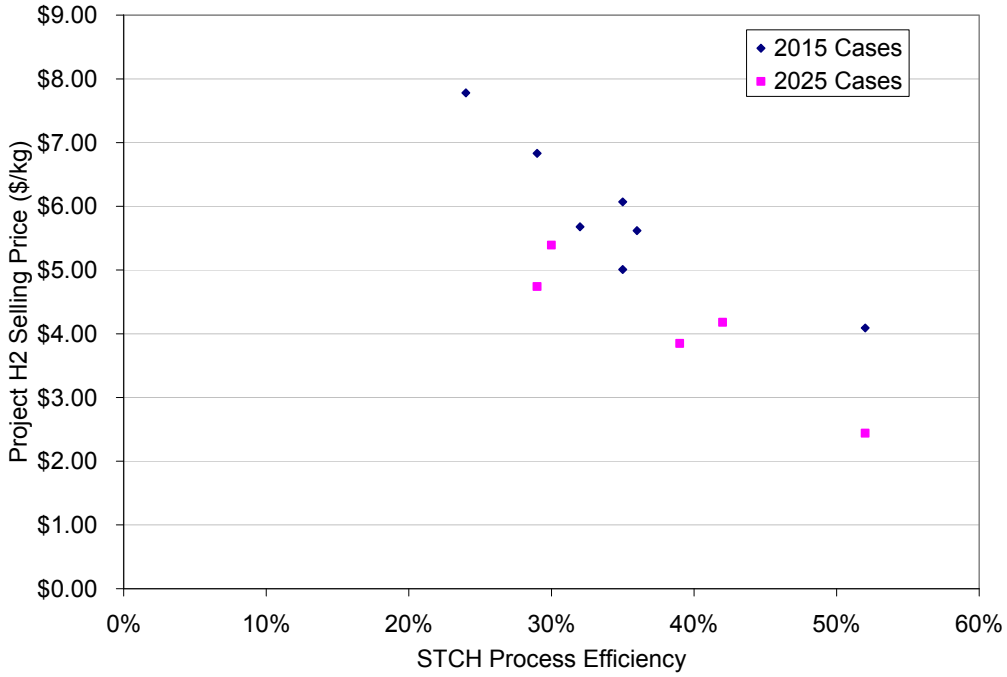

Figure 4-3: Hydrogen selling price vs STCH Efficiency

2. The three hybrid processes (S-A, CuCl, and HyS) all face similar challenges with respect to increasing process efficiency, demonstrating reaction chemistry, and development of a low-cost durable electrolysis system. However, they tend towards lower reaction temperatures and more widely used and widely available processes and equipment – suggesting that the technical risks may be lower and scaling production less challenging.
3. The four high-temperature processes (CdO, MnO, ZnO, and Ferrite) face similar challenges with respect to development of high temperature receiver/reactors, minimizing back reactions, and demonstrating cycle kinetics. These systems tend to have high process efficiency, which suggests that if they are feasible, they will have favorable economics.

While several of the cycles that were evaluated appear likely to achieve the near-term DOE target of $6/kg hydrogen (production only), achieving the long-term goal of $2 to $3/kg hydrogen (delivered) appears to be a very challenging prospect. Of the cycles evaluated, only one (the thin film ferrite cycle) is projected to achieve the target using base case assumptions. Even in this case, achieving the long-term target requires significant technological development along multiple dimensions, as well as demonstration and scale up of novel chemical plant

concepts. Single-variable sensitivity analysis indicates that several other processes could also approach this target if more favorable economic or operational assumptions are used. While specific sensitivities vary between cycles, the plant's capacity factor, the specific economic assumptions used,[45] the cycle efficiency, and the direct capital cost were all shown to have a large effect on plant economics for each of the cycles.

[45] i.e., standard H2A financial parameters as compared to the financial parameters used in the Sargent & Lundy 2003 study [4], which is reflective of solar industry standard practice

References

1. Perret, R. "Development of Solar-Powered Thermochemical Production of Hydrogen from Water." DOE Hydrogen Program, FY 2008 Annual Progress Report, Pp 245-253. Contract #DE-FG36-03GO13062. 2008.
2. Department of Energy Hydrogen Program. "DOE H2A Analysis Assumptions and Ground Rules." Available online at http://www.hydrogen.energy.gov/h2a_prod_rules.html.
3. Department of Energy Hydrogen Program. "Fuel Cell Technologies: Multi-Year Research, Development and Demonstration Plan." Technical Plan, Section 3.1. 2007. Available online at http://www1.eere.energy.gov/hydrogenandfuelcells/mypp/
4. Sargent and Lundy, "Assessment of Parabolic Trough and Power Tower Solar Technology Cost and Performance Forecasts". NREL, NREL/SR-550-34440, October 2003.
5. Turton, R, Bailie, R, Whiting, W, and Shaeiwitz, A. Analysis, Synthesis, and Design of Chemical Processes. 2nd Edition. New Jersey: Prentice Hall. 2003
6. Kolb, G, Jones, S, Donnelly, M, Gorman, D, Thomas, R, Davenport, R, and Lumia, R. "Heliostat Cost Reduction Study". Sandia National Laboratories, SAND2007-3293. June, 2007.
7. Gorensek, M., et. al. "Conceptual Design for a Hybrid Sulfur Thermochemical Hydrogen Production Process," Savannah River National Laboratory. Presented at the 2005 ANS Annual Meeting, San Diego, CA. June 2005.
8. Buckner, M, et. al. Conceptual Design for a Hybrid Sulfur Hydrogen Production Plant. Savannah River National Laboratory, WSRC-TR-2004-00460. April 2005.
9. Gorensek, M and Summers, W. "Hybrid Sulfur flowsheets using PEM elelctrolysis and a bayonet decompostion reactor." International Journal of Hydrogen Energy, Vol. 34, No. 9, 2009.
10. Gorensek, M, Summers, W, Bolthrunis, C, Lahoda, E, Allen D, and Greyvenstein , R. "Hybrid Sulfur Process Reference Design and Cost Analysis." Savannah River National Laboratory. Prepared for the U.S. Department of Energy, Contract #DE-AC09-08SR22470. June 2009.
11. Summers, W. Corgnale, C. "H2A Report HyS cycle." Savannah River National Laboratory. 2008
12. Kistler, B. L. A User's Manual for DELSOL, SAND86-8018, November 1986.
13. Summers, W, Corgnale, C. "Hydrogen Production via Solar Water-Splitting Using the Hybrid Sulfur Process." 2009 AIChE Spring Meeting, Tampa, FL. April 2009.
14. Summers, W. Corgnale, C. "White Paper for Down Select Meeting: Status of the Hybrid Sulfur Cycle." Savannah River National Laboratory. White Paper for the 2008 STCH Down-Select Meeting. October 2008.
15. Summers, W. "Hybrid Sulfur Thermochemical Cycle." Savannah River National Laboratory. DOE Hydrogen Program 2009 Annual Merit Review. May 2009.
16. Falcone, P. K., et. al. "Assessment of a Solid Particle Receiver for a High Temperature Solar Central Receiver." Sandia National Laboratories, SAND85-8208. Feb 1985.
17. Herrmann, U, Geyer, M, and Kearney, D. "Overview on Thermal Storage Systems." FLABEG Solar International GmbH. Workshop on Thermal Storage for Trough Power Systems. February 2002
18. Kearney, D. "Assessment of Thermal Energy Storage for Parabolic Trough Solar Power Plants." Kearney & Associates.

19. Mancini, T. "Power Tower Road Map Meeting and Preliminary Results." Sandia National Laboratories. April 2010.
20. Lewis, M. "Final 9-30 White Paper for STCH." Argonne National Laboratory. White Paper for the 2008 STCH Down-Select Meeting. September 2008.
21. Lewis, M, Masin, J, Vilim, R, and Serban, M. "Development of the Low Temperature Cu-Cl Thermochemical Cycle." Argonne National Laboratory. June 2005.
22. Lewis, M. "Overview/Critical Path in the Cu-Cl Thermochemical Cycle." Argonne National Laboratory. STCH Meeting Presentation, Boulder, CO. October 2010.
23. Tatterson, D. CuCl 2015 and 2025 H2A Production Case Study Spreadsheets. Jan 2011.
24. CAPCOST software developed by R. Turton et. el. and described in Analysis, Synthesis and Design of Chemical Processes (2 ed), Prentice Hall, 2003.
25. Correspondence with Steven Pew and Pat Walsh of Porcelain Industries, Inc. of Dickson, TN, April 2007.
26. Channel, M, Lewandowski, A, and Weimer, A. "Solar-thermal Water Splitting with 5 nm NiFe2O4 on ZrO2 Supports: Process Development & H2A Analysis." University of Colorado. February 2011.
27. T. Wendelin, "SolTRACE: A New Optical Modeling Tool for Concentrating Solar Optics," Proceedings of the ISEC 2003: International Solar Energy Conference, 15-18 March 2003, Kohala Coast, Hawaii. New York: American Society of Mechanical Engineers; pp. 253-260, NREL Report No. CP-550-32866 (2003).
28. Lewandowski, A. "Overview of Solar Thermal Collector Field Design." National Renewable Energy Laboratory. October 2009.
29. Martinek, J, Channel, M, Lewandowski, A, and Weimer, A. "Considerations for the Design of Solar-Thermal Chemical Processes." Journal of Solar Energy Engineering. Vol. 132. August 2010.
30. Channel, M, Scheffe, J, Lewandowski, A, and Weimer, A. "5nm NiFe2O4 on ZrO2 Solar thermal Water Splitting: In progress Process Development and H2A Analysis." University of Colorado. STCH Meeting Presentation, Boulder, CO. October 2010.
31. Correspondence with Al Weimer and Melinda Channel, Dec 2010
32. Davenport, R. Sulfur-Ammonia 2015 and 2025 H2A Production Case Study Spreadsheets. Jan 2011.
33. Genders, D and Symons, P. "Electrolysis of Ammonium Sulfite." Electrosynthesis Company, Inc. STCH Meeting Presentation, Boulder, CO. October, 2010.
34. Weimer, A, Perkins, C, Lichty, P, Funke, H, Zartman, J, Hirsch, D, Bingham, C, Lewandowski, A, Haussener, S, and Steinfeld, A. "Development of a Solar-thermal ZnO/Zn Water-splitting Thermochemical Cycle." University of Colorado. Final Report to the Department of Energy, DE-PS36-03GO93007. April 2009.
35. NREL Solar Field Analysis. Appendix G, Solar Hydrogen Generation Research (SHGR). http://shgr.unlv.edu/
36. Zartman, J, and Perkins, C. "Solar H2 Production via the Zn/ZnO Thermochemical Cycle." University of Colorado at Boulder. August 2004.
37. Peters, M and Timmerhaus, K. Plant Design and Economics for Chemical Engineers. 5th edition. New York: McGraw-Hill, Inc., 2003.
38. Weimer, A et al. "H2A Analysis for the Manganese Oxide based Solar Thermal Water Splitting Cycle." University of Colorado. White Paper for the 2008 STCH Down-Select Meeting. October 2008.
39. Correspondence with Al Weimer, Jan 2011.

40. Wong, B et al. "Cadmium Oxide Solar Thermochemical Hydrogen Cycle." General Atomics. White Paper for the 2008 STCH Down-Select Meeting. October 2008.
41. Wong, B, Brown, L, Buckingham, B, Rennels, R, and Chen, Y. "Solar Cadmium Hydrogen Production Cycle." General Atomics. DOE Hydrogen Program Annual Merit Review. May 2009.
42. Epstein, M and Segal, A. "High efficiency generation of hydrogen fuel using solar thermochemical splitting of water – Solar Optics Design and Cost Data." Weizmann Institute. Final Report to General Atomics. July 2008.
43. Technology Insights. "Framework for Economic Evaluation of Nuclear Hydrogen Production." Technology Insights. Prepared for Sandia National Laboratories, Contract 644343. September 2007.
44. Brown, L. C., et. al., High Efficiency Generation of Hydrogen Fuels Using Nuclear Power, NERI Grant # DE-FG03-99SF21888, GA-A24285, Rev 1, December 2003.
45. Buckingham, B. "Solar powered hydrogen production via the Sulfur-Iodine cycle." General Atomics. White Paper for the 2008 STCH Down-Select Meeting. October 2008.
46. Pickard, P. "Sulfur-Iodine Thermochemical Cycle." Sandia National Labs. 2008 DOE Hydrogen Program Annual Merit Review. June 2008.
47. James, B, Kalinoski, J, and Baum, K. "Mass-Production Cost Estimation for Automotive Fuel Cell Systems." Directed Technologies, Inc. Hydrogen Program Annual Merit Review, June 2010.
48. matche.com Equipment cost database. http://matche.com/EquipCost/index.htm
49. Vendor quote for Saint Gobain Hexoloy silicon carbide tubes.

Appendix A: STCH H2A Assumptions

Table A-1: STCH H2A Financial Assumptions

Category	Value	Justification
Reference $ Year	2007	DOE Guidance
After-Tax Real IRR (%)	10%	H2A Default
Depreciation Type (MACRS, Straight Line)	MACRS	H2A Default
Depreciation Schedule Length (No. of Years)	20	H2A Default
Analysis Period (years)	40	H2A Default
Plant Life (years)	40	H2A Default
Assumed Inflation Rate (%)	1.90%	H2A Default
State Income Taxes (%)	6.0%	H2A Default
Federal Income Taxes (%)	35.0%	H2A Default
Effective Tax Rate (%)	38.9%	Calculated
% Equity Financing	100%	H2A Default
% Debt Financing	0%	H2A Default
Debt Period (years)	0	H2A Default
Interest Rate on Debt, if applicable (%)	0.0%	H2A Default
Length of Construction Period (years)	3	STCH team discussion
% of Capital Spent in 1st Year of Construction	10%	STCH team discussion
% of Capital Spent in 2nd Year of Construction	25%	STCH team discussion
% of Capital Spent in 3rd Year of Construction	65%	STCH team discussion
Start-up Time (years)	0.5	Wind & biomass H2A case study
% of Revenues During Start-up (%)	50%	Wind & biomass H2A case study
% of Variable Operating Costs During Start-up (%)	75%	Wind & biomass H2A case study
% of Fixed Operating Costs During Start-up (%)	100%	Wind & biomass H2A case study
Working Capital	15%	H2A Default
Salvage Value of Capital (% of Total Capital Investment)	10%	H2A Default
Decommissioning Costs (% of Depreciable Costs)	10%	H2A Default

Table A-2: Inflation adjustment factors

Category	Price Adjustment
Direct plant capital costs	Chemical Engineering Plant Cost Index (CEPCI)
Labor Costs	Employee Cost Index (ECI)
Electricity Costs	Producer price index (PPI) for electricity costs.
Other	Consumer price index (CPI)

Table A-3: STCH Solar Plant Direct Capital Cost Assumptions

Category	Guideline	Source
Heliostats - 2015	$127/m^2	Sandia heliostat cost reduction study [6]
Heliostats - 2025	$90/m^2	Sandia heliostat cost reduction study [6]
Tower	795e3 + 23.5 * (ht, m)$^{2.4}$	S&L [4] - Table B-1, escalated to 2007$
Thermal storage	$20/kWh$_{th}$	Sandia roadmap target [19]
Controls	$2.1M	S&L [4], Table E-2, escalated to 2007$
Balance of plant	22.5 x (Plant Size (MWth)/469)$^{0.7}$	Half of S&L estimate, which includes a steam turbine balance of plant, scaled according to avg plant thermal capacity and escalated to 2007$

Table A-4: STCH Solar & Chemical Plant Indirect Cost Assumptions

Category	Solar		Chemical	
	Guideline	Source	Guideline	Source
Site Preparation	9.9M x (Field area (m2)/2.67e6)	S&L, Table E-2 [4]: Escalated by general CEPCI factor from 2002 to 2007$ and scaled linearly according to field size	Varies	For standard capital equipment (e.g., CapCost), already included in the installation factor. Case-by-case basis otherwise.
Engineering & design ($)	17.8% of direct capital	S&L, Table E-2 [4]	Varies	For standard capital equipment (e.g., CapCost), already included in the installation factor. Case-by-case basis otherwise.
Process contingency ($)	N/A	Included w/project contingency	N/A	Included w/project contingency
Project contingency ($)	16.7% of direct capital	S&L, Table E-2 [4], average of all cases	18%	From Brown, L. C., et. al., Table 3-13 (NERI Report) [44]
Up-front permitting costs ($)	3% of direct capital	STCH team guidance	Same as solar	Same as solar
Land Use	Varies	Calculate from heliostat area and estimated packing density	Varies	Estimate on a case-by-case basis – typically much smaller than solar.
Land cost	$2,024 per acre	$5,000 per hectare - from S&L - Table E-2 (2.47 hectares/acre); lower than H2A default because low-cost dessert land is used	Same as solar	Same as solar

Table A-5: STCH Solar & Chemical Plant O&M Cost Assumptions

Category	Guideline		Source/Notes
	Solar	Chemical	
Labor rate	$31/hr burdened rate	$50/hr	**Solar:** From S&L, Table 5-19: $25/hr burdened rate, inflated form 2002$ to 2007$ using the Employment Cost Index **Chemical:** H2A default
Staffing	0.016 staff /1000 m^2 field size	$(6.20 + 31.7\ p^2 + .23N)^{0.5}$ (*See Note)	**Solar:** S&L [4], App G. Includes maintenance staff only, scaled linearly based on the size of the solar field. Administrative & plant operators are included in the chemical plant staff. **Chemical:** Turton, Eq 6.3 [5]
G&A Rate	20%	20%	H2A Default
Property Tax & Insurance	1%	2%	**Solar:** S&L, table B-4 [4]. 0.5% each for insurance, 0.5% for property tax. **Chemical:** H2A default
Material costs for maintenance and repairs ($/year)	0.5% of direct capital cost	In general, 6% of capital costs; adjust on a case-by-case basis	**Solar:** S&L - Table G-5; varies, but 0.5% is used for most solar field components. **Chemical:** Turton (Table 6.2) [5]
Fuels/feedstocks	N/A	Varies	In general - H2A default; cooling water - use S&L value of 0.32/m3 (desert)
Cost of Electricity – 2015	N/A	$83.4/MWh	S&L costs for Solar 100, inflated to 2007$ (PPI) and adjusted for 2015 heliostat cost
Cost of Electricity – 2025	N/A	$58.5/MWh	S&L costs for Solar 220, inflated to 2007$ and adjusted for 2025 heliostat cost[46]
By-Product Credits	N/A	$0	No by-product credits allowed – DOE STCH guidelines
Solar auxiliaries - for systems w/thermal storage	5 MW_e x ($MW_{th,\ peak}$/1,400)	N/A	Scales w/half of S&L [4] estimate, which includes a power generation block
Solar auxiliaries – no thermal storage	0.2 W/m^2	N/A	Based on field measurements for heliostat tracking energy use [29]
Replacement Costs (General)	0.5% of capital	Same as Solar	Common H2A assumption (e.g., biomass, coal case studies), , w/ adjustments on a case-by-case basis

*P is the number of processing step involving handling of particulate solids, and N is the number of nonparticulate processing steps. N is generally the sum of the total pieces of equipment (compressors, towers, reactors, etc).;

[46] S&L heliostat costs are slightly higher than 94 vs $90/m2) than the 2025 plant).

Appendix B: STCH Solar Field Efficiency Analysis Guidelines

A summary of the factors that contribute to solar field and receiver losses is included is shown in Table B-1. Several of these factors are proscribed (as shown in the third column). The other factors are dependent on the solar field and receiver design, and represent the outcome of a complex optimization process. These should be determined using a solar field optimization tool.

Table B-1: Solar field loss mechanisms

Loss Mechanism	Description	Efficiency
Solar Field Losses		
Mirror reflectance	Absorption of solar energy by the mirrors	94% [S&L]
Mirror cleanliness	Soiling of mirrors	95% [S&L]
High wind outage	Time that solar collection is off-line due to high wind.	99% [S&L]
Heliostat field availability	Time that collectors are off-line for maintenance, etc	99.5% [S&L]
Cosine losses	Angle of incidence between the sun and the receiver	Varies with field design
Shading and blocking	Shading of solar collectors (e.g., other collectors, the tower)	Varies with field design
Atmospheric attenuation	Attenuation in thermal energy as it is transmitted from collectors to the receiver	Varies with field design
Receiver Aperture Intercept ("Spillage")	Focused energy that does not intercept the receiver	Varies with field design and receiver properties
Receiver Losses		
Absorptance	Reflection of thermal energy by the receiver	Varies with receiver design
Radiation & Convection	Radiation and convection of thermal energy from the receiver to the environment	Varies with receiver design
Storage/Piping	Energy loss from storing and transporting the working fluid	Varies with thermal storage

Appendix C: Electrolyzer Cost Basis

Electrolyzer module costs were estimated using the module component cost estimates from DTI's bottom-up automotive PEM fuel cell manufacturing cost model developed for the DOE hydrogen [47] as a guideline. The estimates include higher assembly costs than those assumed in the DTI automotive analysis, which reflects the more labor-intensive assembly process associated with the large-format electrolysis units used in STCH plants. Individual components of the electrolyzer module are estimated on a cost-per-unit area basis. The total module cost is then calculated based on the gross active area needed to achieve the required net power output, which is a function of the assumed current density (100 to 500 mA/cm^2, depending on the specific case in question) , cell voltage (0.5 to 0.7 V), and the current efficiency (88% to ~100%). For the 2015 case, the DTI estimates for a production volume of 30,000 vehicles per year were used; for the 2025 case, the 80,000 vehicles per year estimate were used. On an active area basis, 30,000 vehicles per year corresponds to approximately 8 STCH plants, while 80,000 vehicles per year would correspond to approximately 20 STCH plants.

The balance of the electrolysis system includes elements such as power electronics, feed pumps and processing equipment, piping, pressure vessels (as needed), and building space [10]. The hybrid-sulfur analysis includes these elements as a lump sum, whereas the CuCl and sulfur-ammonia cases include some elements elsewhere in the cost analysis, and some of these elements as part of the module cost. After careful review of each case, it appears that these elements are consistently accounted for across the different case studies.

A summary of the electrolyzer module and balance-of-system cost contributors is shown in Table C-1.

Table C-1: Electrolyzer module costs. Source: DTI 2010 AMR presentation [47], slide 35. 2015 costs reflect 30K volume; 2025 costs reflect 80K volume.

Component	Cost ($/m2)		Notes
	2015	2025	
Module			
Electrocatalyst	Depends on precious metal loading		$1,110/troy oz (Pt 5-yr avg) $335/troy oz (Pd 5-yr avg)
Bipolar plates	$44.2	$44.9	DTI Bipolar plates
Electrodes	$105	$64.8	DTI GDL cost, adjusted for specific cases
Membrane	$94.7	$58.2	DTI Nafion membrane
Structural material (cells)	$38.4	$36.5	Includes gaskets, end plates, current collectors, compression bands & MEA housing from DTI
Assembly costs	$59	$59	Cells + Modules: TIAX estimate
Balance of Plant			
Pressure Vessel	Varies		Depends on process conditions
Power Electronics	$312	$312	Power supply, rectifiers, DC bus controls. Based on vendor quote.
Feed pumps	Varies		Depends on flow rates, processing equipment, etc
Other	Varies		Includes piping, etc
Installation Factor	**1.2**	**1.2**	Consistent with central electrolysis H2A case study